ELECTRONIC SUPPLEMENTARY INFORMATION

A flexible self-folding receptor for coronene

David Lozano, Rubén Álvarez-Yebra, Ricard López-Coll, Agustí Lledó.*

Institut de Química Computacional i Catàlisi (IQCC), and Departament de Química
Universitat de Girona, c/Maria Aurèlia de Capmany 69, 17003 Girona, Spain.

* agusti.lledo@udg.edu

Table of Contents

1 Materials and methods

Unless otherwise noted, materials were obtained from commercial suppliers and used without further purification. Dichloromethane (DCM) and tetrahydrofuran (THF) were degassed and dried under nitrogen by passing them through a solvent purification system (MBraun, SPS-800). Reaction progress was monitored using thin layer chromatography (TLC) on Macherey-Nagel Xtra SIL G/UV254 silica gel plates. Flash column chromatography was performed on silica gel 60 (40-60 μm SiO_2). IR spectra were recorded on an Agilent Cary 630 FT-IR spectrometer equipped with an ATR sampling accessory. ^{1}H and ^{13}C NMR spectra were recorded at 298 K unless otherwise stated, at 400 MHz and 101 MHz respectively. A Bruker Ultrashield AVANCE III 400 spectrometer equipped with a 5 mm BBI probe and a Bruker ASCEND 400 spectrometer equipped with a 5 mm BBFO probe were used. NMR spectra were internally referenced to tetramethylsilane (^{1}H) or, alternatively, to the residual proton solvent signal (^{13}C). The NMR data are reported as follows: chemical shift (δ) in ppm from tetramethylsilane, multiplicity (br = broad, s = singlet, d= doublet, t = triplet, q = quartet, m = multiplet), coupling constants (Hz), integration (^{1}H) and assignment. High resolution mass spectra (HRMS) were recorded on a Bruker micrOTOF-QII instrument with an ESI source. Samples were introduced into the mass spectrometer ion source by direct infusion through a syringe pump and were externally calibrated using sodium formate.

2 Synthetic procedures

8-amino-1-naphthol (3a)

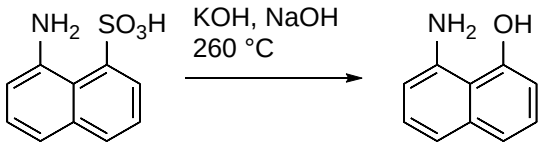

3a

Compound **3a** was prepared according to a reported procedure with minor modifications.[1] 8-Aminonaphthalene-1-sulfonic acid (15 g, 67.2 mmol) is made into a paste with H_2O (18 mL). KOH (26.4 g, 472 mmol) and NaOH (26.4 g, 660 mmol) are melted at 200 °C in a stainless steel 500 mL beaker employing a mechanical stirrer. The 8-Aminonaphthalene-1-sulfonic acid paste is added in portions with continuous stirring of the mixture. The temperature is slowly increased to 260 °C while stirring. When the temperature reaches 260 °C, the mixture turns dark brown. The mixture is kept for additional 15 min. at this temperature, and then rapidly cooled using a water bath. The solidified cake is dissolved in H_2O (500 mL) with stirring, and filtered through Celite in a Büchner funnel (using a #3 Whatman filter paper as support) to remove the black tarred material formed. The filtrate is acidified with conc. HCl to pH ~ 1, and filtered again through Celite to remove any remaining solid. The filtrate is neutralized in an Erlenmeyer flask by adding solid $NaHCO_3$ under stirring, and then extracted with EtOAc (3 x 80 mL).* The combined organic layers are washed with brine (200 mL), dried (anh. Na_2SO_4), filtered, and concentrated *in vacuo* to give a green solid (5.71 g, 53% yield) corresponding to 8-amino-1-napthol **3a**.

**In the original procedure the precipitated aminonaphthol is directly isolated by filtration from the acidified suspension. We found the product obtained in this manner to be quite unstable, even when stored cold under nitrogen. The product isolated by extraction is equally pure and considerably more stable; it can be stored under nitrogen in the fridge for months without apparent degradation.*

2.1 Calix[5]arene pentaacid 2.

Calix[5]arene pentaacid **2** has been previously reported. Herein we present a detailed 5-step synthetic sequence based on reported procedures that has produced the best overall yields in our hands (Scheme S1).[2]

Scheme S1. Detailed synthetic sequence for calix[5]arene pentaacid **2**.

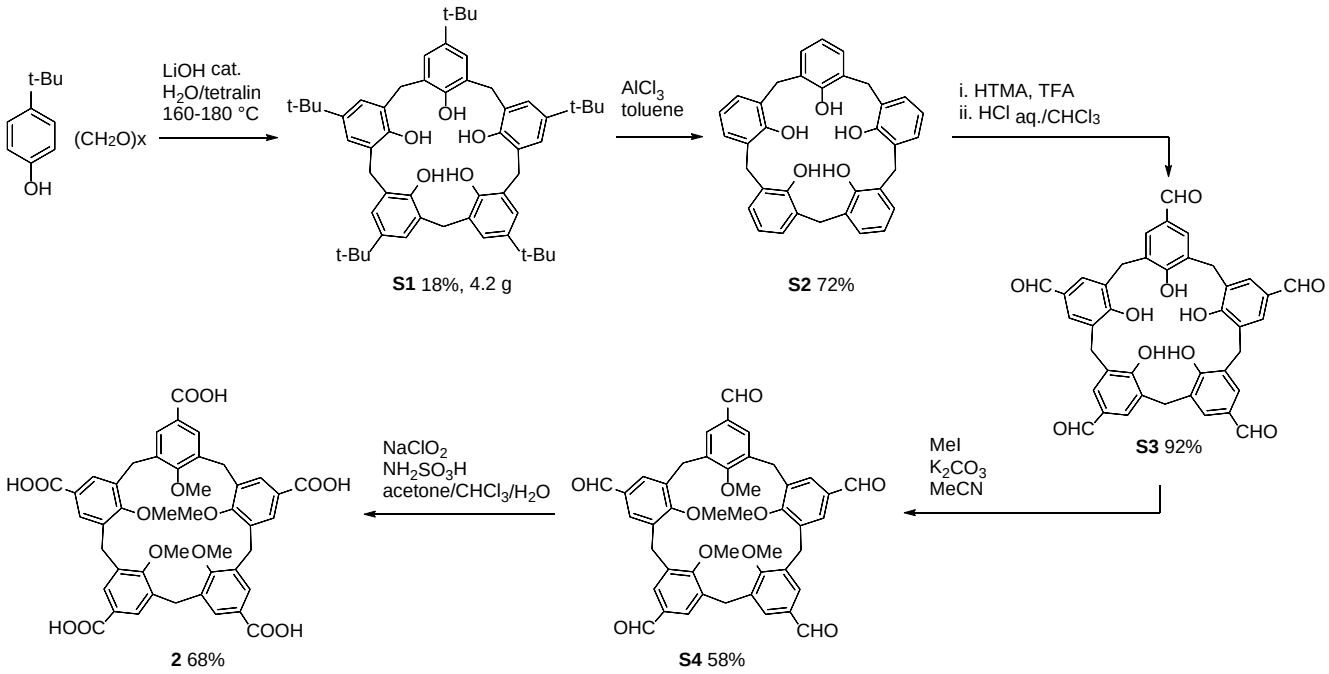

5,11,17,23,29-Penta(tert-butyl)-31,32,33,34,35-pentahydroxycalix[5]arene (S1)

The experimental procedure was adapted and scaled down from that described by Gutsche.[2c] In a 3-necked 500 mL round bottom flask was placed 4-*tert*-butylphenol (20.25 g, 135 mmol) and paraformaldehyde (13.52 g, 450 mmol). The reaction flask is equipped with a 4 cm oval magnetic stirrer, a Dean-Stark receiver, a condenser, a gas inlet connected to a nitrogen manifold, and a thermometer/adaptor set for monitoring the inner temperature (Fig. S1). A gas outlet (oil bubbler) is connected at the end of the condenser following the Dean-Stark. The system is placed on a hotplate stirrer equipped with an aluminum block for rapid heating. The thermocouple of the hotplate is inserted in the aluminum block. The distillation path of the Dean-Stark is covered with insulating material covered in aluminum foil. The whole upper body of the flask is also insulated when temperatures above 180 °C need to be sustained along the process. Tetralin (1,2,3,4-tetrahydronaphthalene, 270 mL) is then added and the system is flushed with nitrogen. A solution of LiOH (976 mg, 40.8 mmol) in H_2O (9.5 mL) is added at once. A gentle flow of nitrogen is maintained. The slurry is stirred magnetically (600 rpm) and the temperature of the hotplate/block is set to 95 °C; within 15-30 min the inner temperature reaches 80-85 °C. The mixture is kept at 85 °C for 1.5 h, during which time the mixture turns pale yellow. At this point the upper body of the flask is covered with the insulating layer and the hotplate is set to 230 °C. When the inner temperature reaches 185-190 °C (5 min) the mixture is stirred for further 10 min at this temperature. After this period, around 13 mL of water have been collected on the Dean-Stark apparatus. At this point the temperature of the hotplate is set to 180 °C and the insulating layer is removed, causing the inner temperature to drop to 160 °C. The mixture is stirred at 160 °C for 3 h and then let to cool down. The cold slurry is filtered through a #4 fritted funnel. The solids are rinsed with toluene and discarded. The filtrate is concentrated under reduced pressure in a rotary evaporator. A conventional diaphragm pump is sufficient to remove most of the toluene, tetralin can be removed by switching to a high vacuum pump (ca 1 mmHg) and heating to 70 °C. The use of an insulated

adaptor facilitates this process. Complete removal of tetralin is done on a high vacuum manifold, heating with a heat gun until the sticky oil becomes foam-like. This step is important because residual tetralin hampers crystallization later on. Once cold, the solids are treated with 40 mL of 1M HCl and 70 mL of $CHCl_3$ and stirred vigorously. The resulting biphasic mixture is filtered in a Büchner funnel with a double layer of #3 Whatman paper. The solids are rinsed with $CHCl_3$ until the filtrate is colorless, and discarded. The biphasic filtrate is transferred to a separation funnel and the aqueous phase is further extracted with 40 mL of $CHCl_3$. The combined $CHCl_3$ layers are dried with anh. Na_2SO_4, filtered and concentrated under reduced pressure. The product is thoroughly dried under high vacuum and heating to remove any remaining tetralin at this point. The resulting solids are refluxed with 150 mL of acetone (30 min). The resulting suspension is filtered hot, and the solids are rinsed with 30 mL of fresh boiling acetone. The filtrate is concentrated to ca 45 mL. At this, point small quantities of a fine white powder may appear, and are removed by filtration. Crystallization from the filtrate starts upon cooling in the freezer. The process is facilitated by eventual sonication, and the slurry is left in the freezer overnight. The obtained solids are filtered, rinsed carefully with cold acetone, and dried under high-vacuum. 4.197 g (19%) of the title compound are obtained as a white powder. Spectroscopic data matches the reported values.

Notes:
1. In our experience, the key step of this preparation is the central heating period during which most of the water is removed azeotropically. If this period is sustained for a long time, the yield drops significantly. As a consequence, the scale and the available hardware are critical for the reaction, in order to ensure efficient heat transfer during this step.
2. Discarded solids or mother liquor fractions during the crystallization process with acetone can be checked by TLC for calix[5]arene content (Rf: 0.73 in hexane/acetone 95:5).

Figure S1. Experimental setup used for the preparation of **S1**.

31,32,33,34,35-pentahydroxycalix[5]arene (S2)

Adapted from a reported procedure.[2d] Penta(*tert*-butyl)-calix[5]arene **S1** (3.96 g, 4.88 mmol) is dissolved in 80 mL of anhydrous toluene in a 2-neck RBF under a N_2 atmosphere. $AlCl_3$ (6.46 g., 48.4 mmol, 9.9 eq.) is added in portions, and the resulting mixture is stirred at room temperature. After 3 h, TLC shows almost complete disappearance of the starting material (hexane/acetone 85:15). The reaction is quenched by careful addition of water with cooling in an ice/water bath. When the exothermic reaction ceases, the mixture is stirred for 20 min. with a total amount of H_2O of 160 mL. The phases are separated and the aq. layer is extracted twice with toluene. The combined toluene layers are dried (anh. Na_2SO_4), filtered and evaporated. The resulting solids are triturated in ca 70 mL Et_2O by sonication, filtered, rinsed with fresh

Et_2O and dried under high vacuum. The product is triturated by refluxing in 30 mL of acetone. Upon cooling, the obtained solids are filtered and rinsed with fresh acetone, and dried under high vacuum. A white powder is obtained which corresponds to an acetone solvate (**S2**/acetone 1:2 as ascertained by ^{1}H NMR, 2.276 g, 72% yield). Spectroscopic data matches the reported values.

5,11,17,23,29-Pentaformyl-31,32,33,34,35-pentahydroxycalix[5]arene (S3)

The main limitation of the original procedure, which employs microwave heating, is scalability.[2b] On the other hand, conventional heating requires extended reaction times.[2a] We have found that carrying the reaction on a gram scale in a pressure vessel provides good results in a reasonable time. The calix[5]arene acetone solvate (**2**.$(C_3H_6O)_2$, 1.10 g, 1.70 mmol) and hexamethylenetetramine (HMTA, 9.06 g, 64.6 mmol) are weighed in a pressure vessel (*"250 mL"* Ace Glass 8415-11, actual capacity 200 mL). A rubber septum is adapted and the system purged with N_2. 86 mL of neat TFA are added, and the septum is quickly replaced with the Teflon front-seal threaded plug, equipped with a FETFE O-ring (Sigma-Aldrich) in lieu of the original viton O-ring. The flask is immersed in an oil bath at 125 °C, and the mixture is stirred vigorously for 24 h (adequate shielding is placed in front of the system for safety purposes). After this time, the mixture is let to cool down and transferred to a 1 L flask. 240 mL of $CHCl_3$ and 240 mL of 1M HCl are added and the biphasic mixture is stirred vigorously overnight. The phases are separated, and the aq. layer is extracted with $CHCl_3$ (CAUTION! DO NOT wash the organic layers with water since the product precipitates easily once the organic phase is rinsed from TFA). The combined organic layers are evaporated and fully dried under high vacuum. The resulting solids are triturated with water by sonication in order to remove any remainders of TFA, $NH_4^+Cl^-$ and formaldehyde. The solids are then filtered and thoroughly dried by heating (40 °C) under high vacuum. The product is triturated again in refluxing DCM (30 mL), filtered once cold, and rinsed with DCM. The solids are dried under high vacuum and a fine yellow powder is obtained, which corresponds to the pure product (1.05 g, 92%). Spectroscopic data matches the reported values.

5,11,17,23,29-Pentaformyl-31,32,33,34,35-pentamethoxycalix[5]arene (S4)

S4 was prepared following the reported procedure,[2a] and further purified by flash column chromatography (SiO_2, dichloromethane/EtOAc 95:5 to 90:10). From 638 mg (0.951 mmol) of **S3**, 408 mg of **S4** were obtained (58% yield). Spectroscopic data matches the reported values.

5,11,17,23,29-Pentacarboxy-31,32,33,34,35-pentamethoxycalix[5]arene (2)

In our hands, the previously reported oxidation procedure provided mixtures of compounds and low yields.[2a] We adapted a different procedure employed for calix[4]arene derivaties.[3] We found it important to respect the order in the addition of the reagents, and the use of sulfamic acid in excess over chlorite. In a 250 mL round bottom flask, pentaaldehyde **S4** (409 mg, 0.552 mmol) was dissolved in an acetone/$CHCl_3$ mixture of (3:1, 66 mL). A solution of sulfamic acid (643 mg, 6.62 mmol) in 3.5 mL of H_2O was added. At this point, a solution of sodium chlorite (80%, 499 mg, 4.41 mmol) in 3.5 mL H_2O was slowly added dropwise along 5 min. The resulting pale yellow solution is then further stirred for 24 h at room temperature. After this time the yellow color has faded and the reaction mixture is quenched by addition of 1M HCl (20 mL). The volatiles are then removed under reduced pressure, and a solid precipitates from the aqueous mixture. The suspension is triturated in an ultrasonic bath and the solids are filtered. The obtained solids are dried under vacuum in a desiccator with P_2O_5, resulting in 309 mg of a white powder (68% yield). The ^{1}H and ^{13}C NMR spectra in CD_3OD match the reported data. The ^{1}H NMR spectrum in DMSO-d_6 is reported here for convenience. ^{1}H NMR (400 MHz, DMSO-d_6): δ 12.67 (bs, 5H, COOH), 7.67 (s, 10H, CH), 3.87 (s, 10H, CH_2), 3.21 (s, 15H, CH_3) ppm. ^{1}H NMR (400 MHz, CD_3OD): δ 7.76 (s, 10H, CH), 3.93 (s, 10H, CH_2), 3.29 (s, 15H, CH_3) ppm.

2.2 Synthesis of cavitands 1a-b.

Scheme S2. Synthesis of cavitands

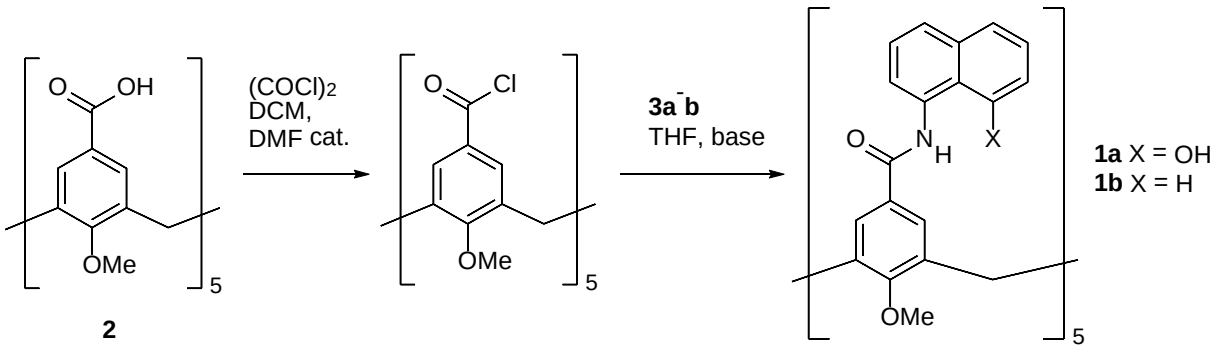

2

Cavitand 1a

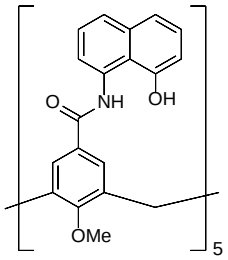

1a

In a round-bottomed flask, calix[5]arene pentaacid **2** (200 mg, 0.244 mmol) was suspended in anh. DCM (22 mL) under a nitrogen atmosphere. Two drops of anh. DMF were added followed by oxalyl chloride (3.67 mL of a 2.0M solution in DCM, 7.31 mmol). The mixture gradually becomes homogeneous, and after stirring for 18 h at room temperature the solvent was removed under reduced pressure. The residue was redissolved in anh. THF (12 mL) and then added dropwise to a solution of aminonaphthol **3a** (388 mg, 2.44 mmol) and anh. pyridine (0.20 mL, 2.44 mmol) in anh. THF (12 mL) The mixture was stirred for 20 h at room temperature under a nitrogen atmosphere. DCM (25 mL) and HCl 1M (15 mL) were then added and the phases separated. The organic layer was washed with water, dried (anh. Na_2SO_4) and concentrated in vacuo to give a green solid crude, which was purified by flash chromatography (SiO_2, eluting first with hexane/EtOAc from 70:30 to 60:40, and then in the same column with $CHCl_3$/EtOH from 99.6:0.4 to 99.5:0.5). The resulting brown solids were dissolved in the minimal amount of $CHCl_3$ and precipitated by addition of *n*-pentane and trituration in an ultrasonic bath. After drying under high vacuum, a pale brown powder corresponding to calix[5]arene **1a** was obtained (171 mg, 46% yield). ^{1}H NMR (400 MHz, $CDCl_3$, 273 K) δ 12.11 (s, 5H, NH), 10.35 (s, 5H, ArOH), 8.70 (d, *J* = 7.6 Hz, 5H, CH), 8.17 (s, 5H, CH), 7.94 (s, 5H, CH), 7.43 (d, *J* = 7.9 Hz, 5H, CH), 7.32 (t, *J* = 7.9 Hz, 5H, CH), 7.23 (d, *J* = 7.7 Hz, 5H, CH), 7.18 (d, *J* = 6.9 Hz, 5H, CH), 7.11 (m, 5H, CH), 4.71 (d, *J* = 12.9 Hz, 5H, CH_2), 3.83 (s, 15H, CH_3), 3.58 (d, *J* = 13.2 Hz, 5H, CH_2) ppm. ^{13}C NMR (101 MHz, $CDCl_3$, 273 K) δ 165.5 (CO), 159.4 (Cq), 152.5 (Cq), 136.1 (Cq), 134.7 (Cq), 134.4 (Cq), 134.3 (Cq), 129.7 (CH), 129.1 (Cq), 126.4 (CH), 126.0 (CH), 125.5 (CH), 124.4 (CH), 120.8 (CH), 116.5 (CH), 115.7 (Cq), 111.2 (CH), 62.0 (CH_3), 28.4 (CH_2) ppm. HRMS (ESI-) m/z calcd. for $C_{95}H_{74}N_5O_{15}^-$ ([M-H]$^-$): 1525.5220; found: 1525.5231. m/z calcd. for $C_{95}H_{73}N_5O_{15}^{2-}$ ([M-2H]$^{2-}$) 762.2573; found: 762.2575. IR v: 3325, 2932, 2693, 1643, 1629, 1547, 1473, 1427, 1300, 1206, 1009, 816, 757 cm^{-1}.

Cavitand 1b

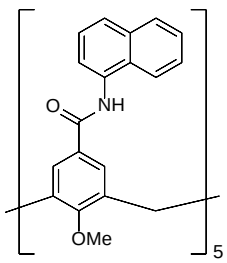

1b

In a round-bottomed flask, calix[5]arene pentaacid **2** (78 mg, 0.0951 mmol) was suspended in anh. DCM (10 mL) under a nitrogen atmosphere. One drop of anh. DMF was added followed by oxalyl chloride (0.24 mL, 2.83 mmol). The mixture gradually becomes homogeneous, and after stirring for 18 h at room temperature the solvent was removed under reduced pressure. The residual compound is dissolved again in dry THF (5 mL). Then, a solution of 1-naphthylamine (**3b**, 81 mg, 0.566 mmol) and anhydrous Et_3N (100 μL, 0.717 mmol) in dry THF (4 mL) is added. The mixture is stirred for 20 h at room temperature under a nitrogen atmosphere. DCM (5 mL) and HCl 1M (3 mL) are added, the aqueous phase is extracted with DCM and the

combined organic layers are washed with water. The organic layer is dried (anh. Na_2SO_4) and concentrated in vacuo to give a green solid crude, which is purified by flash chromatography (SiO_2, DCM/acetone 100:0 to 97:3) to give a brown solid (85 mg, 62% yield) corresponding to calix[5]arene **1b**. An analytically pure sample of **1b** is obtained by sonication of the solid in MeOH (5 mL) to give a pale yellow powder. ^{1}H NMR (400 MHz, $CDCl_3$): δ 8.09(s, NH, 5H), 7,96 (d, 5H, *J* = 7.5 Hz, CH), 7.77 (d, 5H, *J* = 8.1 Hz, CH), 7.64 (s, 10H, CH), 7.62 (d, *J* = 8.6 Hz, 5H, CH), 7.50 (d, *J* = 8.5 Hz, 5H, CH), 7.37 (d, *J* = 8.0, 8.0 Hz, 5H, CH), 7.33 (dd, *J* = 7.6, 7.6 Hz, 5H, CH), 7.23 (d, *J* = 7.0 Hz, 5H, CH), 3.86 (s, 10H, CH_2), 3.38 (s, 15H, CH_3) ppm. ^{13}C NMR (101 MHz, $CDCl_3$): δ 166.3 (CO), 159.4 (Cq), 135.2 (Cq), 134.0 (Cq), 132.7 (Cq), 130.7 (Cq), 128.6 (CH), 128.2 (CH), 127.2 (Cq), 126.2 (CH), 126.0 (CH), 125.8 (CH), 125.7 (CH), 120.8 (CH), 120.6 (CH), 61.4 (CH_3), 30.3 (CH_2) ppm. HRMS (ESI+) m/z calcd. for $C_{95}H_{75}N_5O_{10}Na^+$ ([M+Na]$^+$): 1469.5439; found: 1469.5399. IR ν: 3445, 3152 , 3050 , 2930, 2824, 1666, 1596, 1527, 1496, 1196, 1006, 790, 767 cm^{-1}.

N-(8-hydroxynaphthalen-1-yl)-4-(octyloxy)benzamide (4)

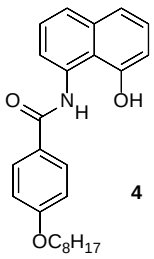

4

In a dry 25 mL round bottom flask, 4-(octyloxy)benzoic acid (75 mg, 0.30 mmol) is dissolved in anh. dichloromethane under a nitrogen atmosphere. Next 1 drop of dimethylformamide is added followed by oxalyl chloride (0.3 mL of a 2M solution in DCM, 0.6 mmol). The solution is stirred at room temperature overnight and then the volatiles are removed under reduced pressure. The resulting solids are redissolved in anh. THF (1 mL) under nitrogen. In a separate flask 8-amino-1-naphthol (**3a**, 46 mg, 0.289 mmol) is dissolved in 2 mL of anh. THF and dry pyridine (25 μL, 0.310 mmol). To this solution is added the acyl chloride solution in THF dropwise, and the resulting mixture is stirred at room temperature for 4 h. Water and ethyl acetate are then added and the mixture stirred for 5 min. The two phases are then separated. The organic layer is washed with more water, dried (Na_2SO_4), filtered, and concentrated under reduced pressure. The crude product is purified by flash column chromatography (SiO_2, hexane/acetone 8:2). The resulting solids are triturated by sonication in DCM/pentane 1:1, filtered, washed with pentane and dried under high vacuum to yield 64 mg of a grey powder (57% yield). ^{1}H NMR (400 MHz, $CDCl_3$) δ 11.42 (s, 1H, NH), 8.85 (d, *J* = 7.3 Hz, 1H, CH), 7.92 (d, *J* = 8.6 Hz, 2H, CH), 7.52 (d, *J* = 8.3 Hz, 1H, CH), 7.49 – 7.40 (m, 2H, CH), 7.26 (m, 1H, CH, overlap w. $CHCl_3$), 7.12 (s, 1H, OH), 6.91 – 6.81 (m, 3H, CH), 3.94 (t, *J* = 6.5 Hz, 2H, CH_2), 1.77 (tt, *J* = 6.7, 6.7 Hz, 2H, CH_2), 1.43 (d, *J* = 8.2 Hz, 2H), 1.39 – 1.18 (m, 8H, CH_2), 0.89 (t, *J* = 7.0 Hz, 3H, CH_3) ppm. ^{13}C NMR (101 MHz, $CDCl_3$) δ 165.6 (CO), 161.9 (Cq), 151.6 (Cq), 136.6 (Cq), 135.4 (Cq), 128.9 (CH), 127.6 (Cq), 126.8 (CH), 125.6 (CH), 123.6 (CH), 122.2 (CH), 116.3 (CH), 115.6 (Cq), 114.4 (CH), 110.8 (CH), 68.2 (CH_2), 31.8 (CH_2), 29.4 (CH_2), 29.24 (CH_2), 29.16 (CH_2), 26.0 (CH_2), 22.7 (CH_2), 14.1 (CH_3) ppm. HRMS (ESI-) m/z calcd. for $C_{25}H_{28}NO_3^-$ ([M-H]$^-$): 390.2075; found: 390.2081. IR ν: 3503, 3055, 2918, 2853, 1627, 1599, 1543, 1501, 1432, 1316, 1251, 814, 758 cm^{-1}.

3 ^{1}H NMR characterization of 1a.

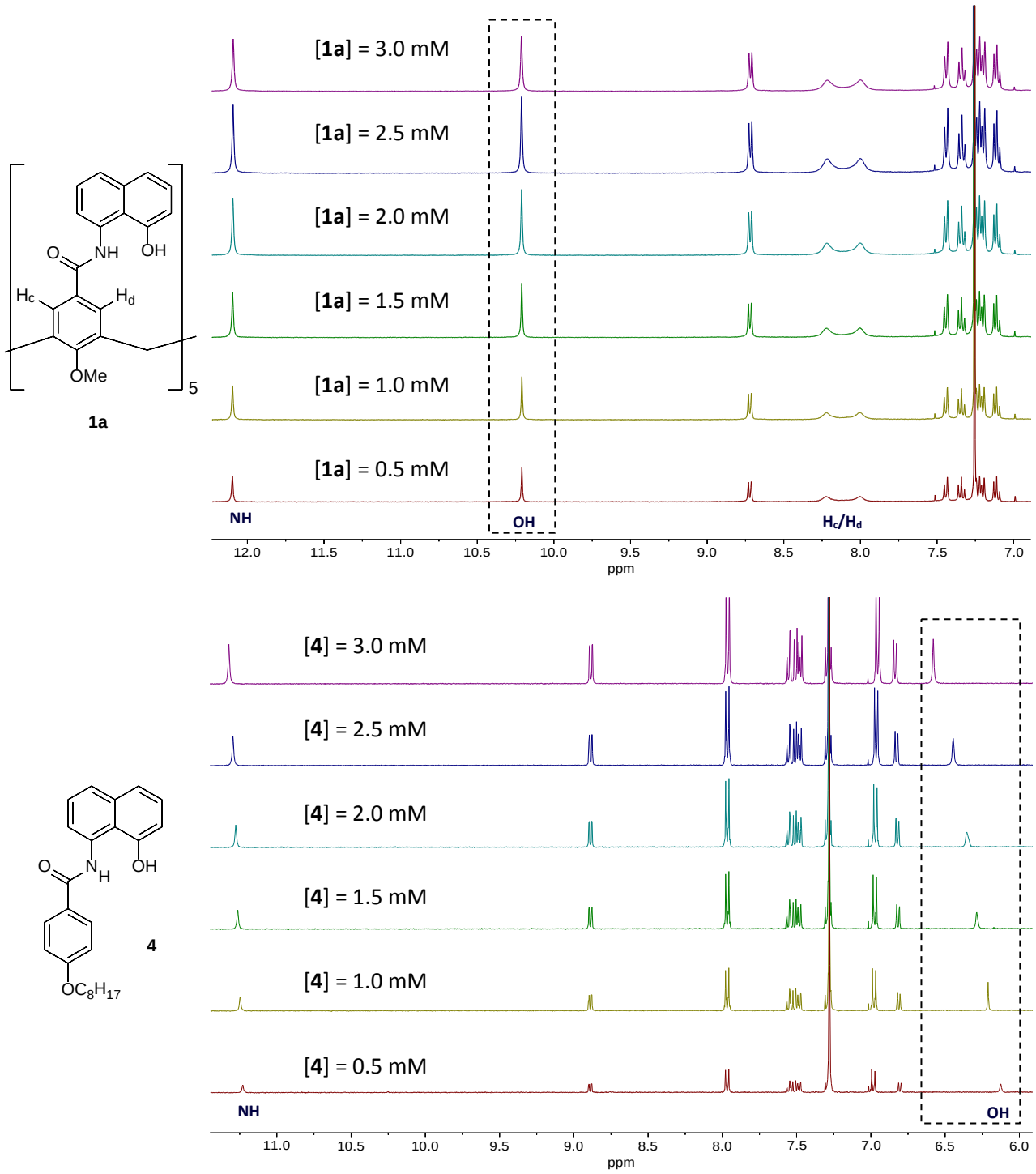

Figure S2. Downfield region of the ^{1}H NMR spectra of **1a**/**4** at different concentrations in $CDCl_3$ (T = 298 K). A significant concentration effect is observed for the OH shift of model compound **4**, but not for **1a**.

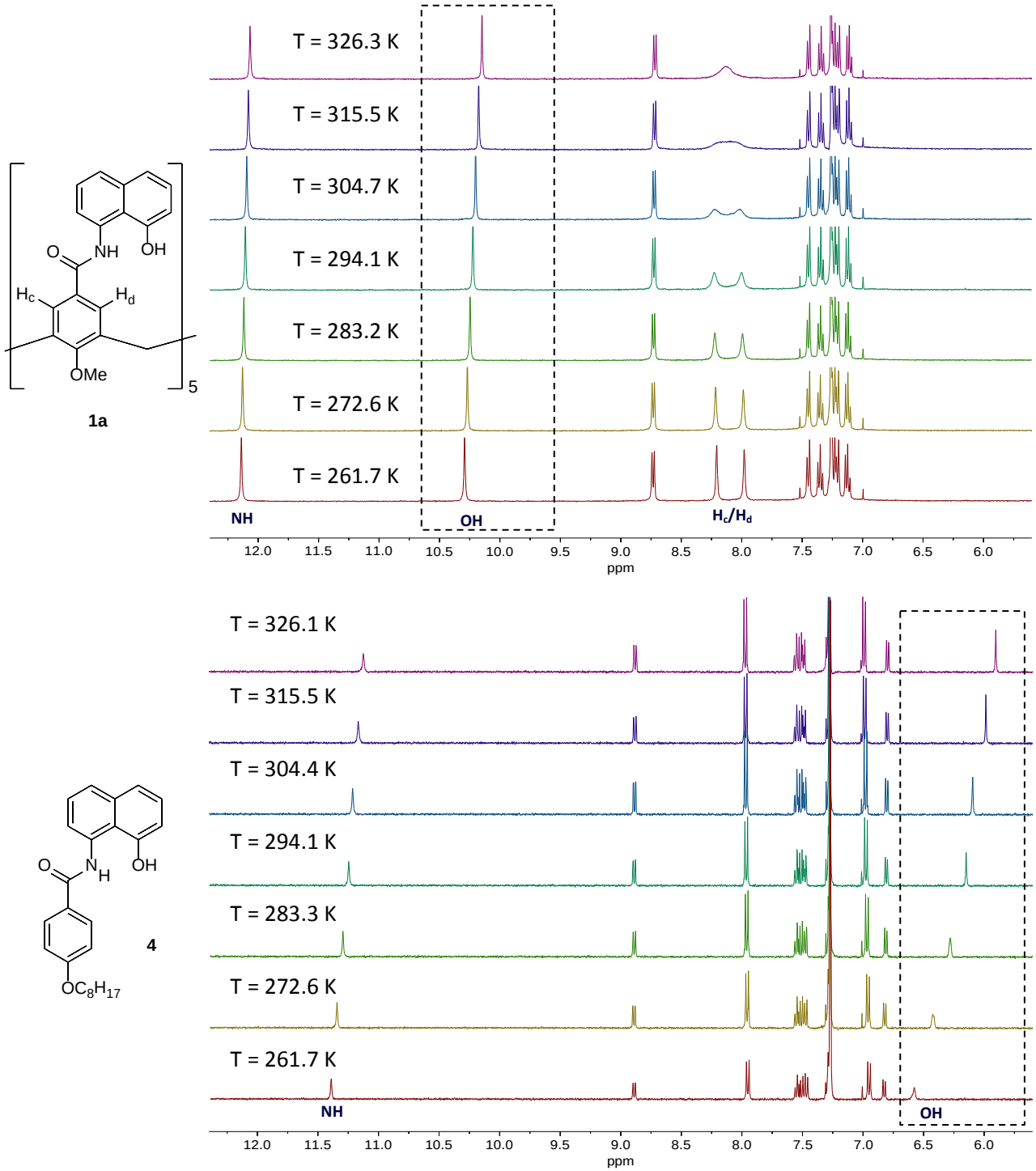

Figure S3. Downfield region of the ^{1}H NMR spectra of **1a**/**4** in $CDCl_3$ at different temperatures ([**1a**] = [**4**] = 1.0 mM).

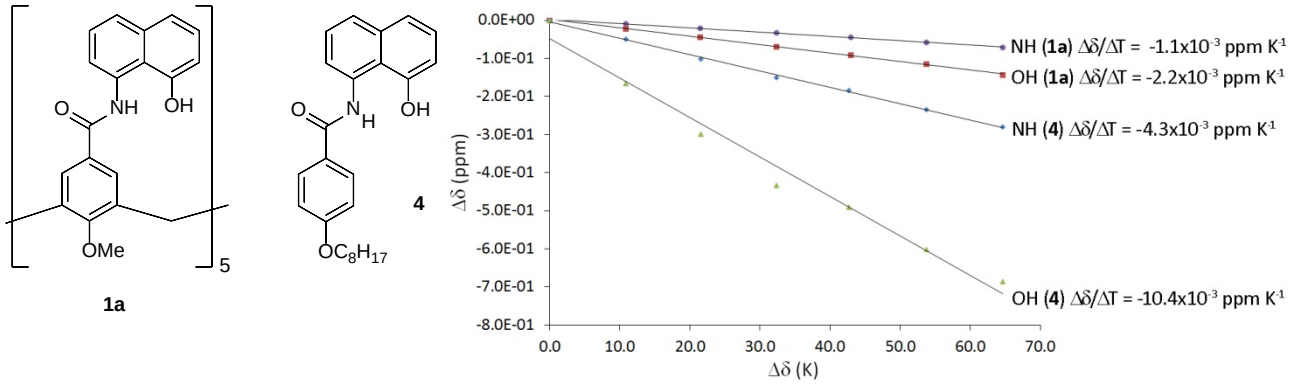

Figure S4. Temperature coefficients ($\Delta\delta/\Delta T$) of NH/OH resonances in **1a**/**4** ($CDCl_3$, [**1a**] = [**4**] = 1.0 mM, T = 263 - 313 K).

3.1 2D NMR EXSY and exchange rate calculations

Two EXSY experiments[4] were carried out at 272.5 K and 299.3 K (in $CDCl_3$) to calculate the aromatic panel rotation and cone flip motions respectively, which occur at different rates. The temperature was controlled by a Bruker BCU-X cooling unit, and was calibrated externally with a CD_3OD standard. For each experiment two ^1H 2D NOESY spectra were acquired sequentially on a sample of **1a** (2.0 mM), one with the desired mixing time (τ_m) and a second reference spectrum at $\tau_m \sim 0$ ms. For acquisition purposes the D8 delay (τ_m) for the second experiment was set to 5 ms. Spectra were recorded using the standard gradient pulsed, phase sensitive NOESY sequence from Bruker (*noesygpph*). Each of the 256 F1 increments was the accumulation of 16 scans. The relaxation delay D1 was set to 4 s. Before Fourier transformation, the FIDs were multiplied by a $\pi/2$ sine square function in both the F2 and the F1 domains.

The rate constants k_1/k_{-1} for the forward and reverse chemical exchange processes were calculated from the integral values of the involved hydrogens (H_a/H_b, H_c/H_d) using the EXSYCalc program (Mestrelab Research).[5] In a system with two exchanging equivalent sites the forward and reverse 1st order reaction rates are the same ($k_1 = k_{-1}$). The integrations of the diagonal peaks should be equal, as well as the two cross-peaks originating from magnetization exchange. The intrinsic uncertainty of the volume integral values obtained from NMR spectra results in slightly different measurements for k_1 and k_{-1}. Rather than artificially equating the integral values, we obtained an estimation of the rate constant k by averaging the measured k_1 and k_{-1} values. We then obtained the corresponding $\Delta G^{\ddagger}$ through the Eyring equation (1). For our dataset, the same $\Delta G^{\ddagger}$ values were obtained by averaging the diagonal and cross-peak integrals and feeding the three unique integration values (diagonal, cross-peaks, and reference diagonal) into EXSYCalc.

$$k = \frac{k_B T}{h} e^{(-\Delta G^{\ddagger}/RT)} \qquad (1)$$

The rate exchange for panel rotation was obtained at 272.5 K to maximize spectral resolution, employing τ_m = 400 ms. For the cone flip motion, chemical exchange evolution and through space cross-relaxation (NOE effect) of the neighboring methylene protons add up. The cross-relaxation component was minimized at 299.3 K and τ_m = 300 ms. Because of its molecular size, cavitand **1a** falls in the region of negative NOE effect, giving rise to diagonal and cross peaks of the same sign (this was corroborated by complementary ROESY experiments). Therefore, any residual NOE contribution will lead to an overestimation of the rate constant. The EXSY calculation will, in the worst case scenario, underestimate the exchange barrier.

In CD_2Cl_2, the panel rotation and cone flip barriers were measured at 250.9 K and 299.4 K respectively.

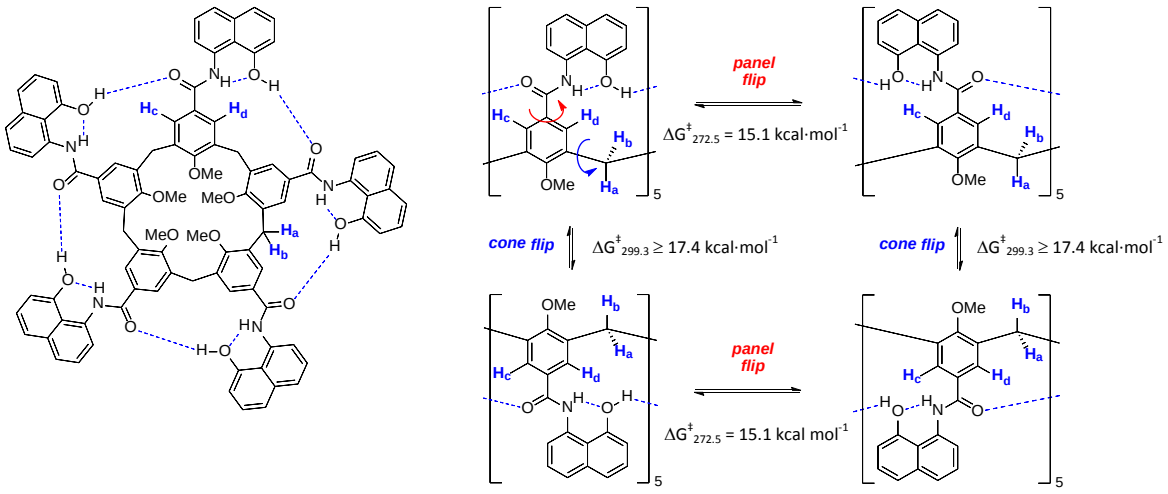

Figure S5. Representation of cone inversion and panel rotation in **1a**, and the associated barriers in $CDCl_3$.

^{1}H 2D EXSY (400 MHz), $CDCl_3$, 299.3 K

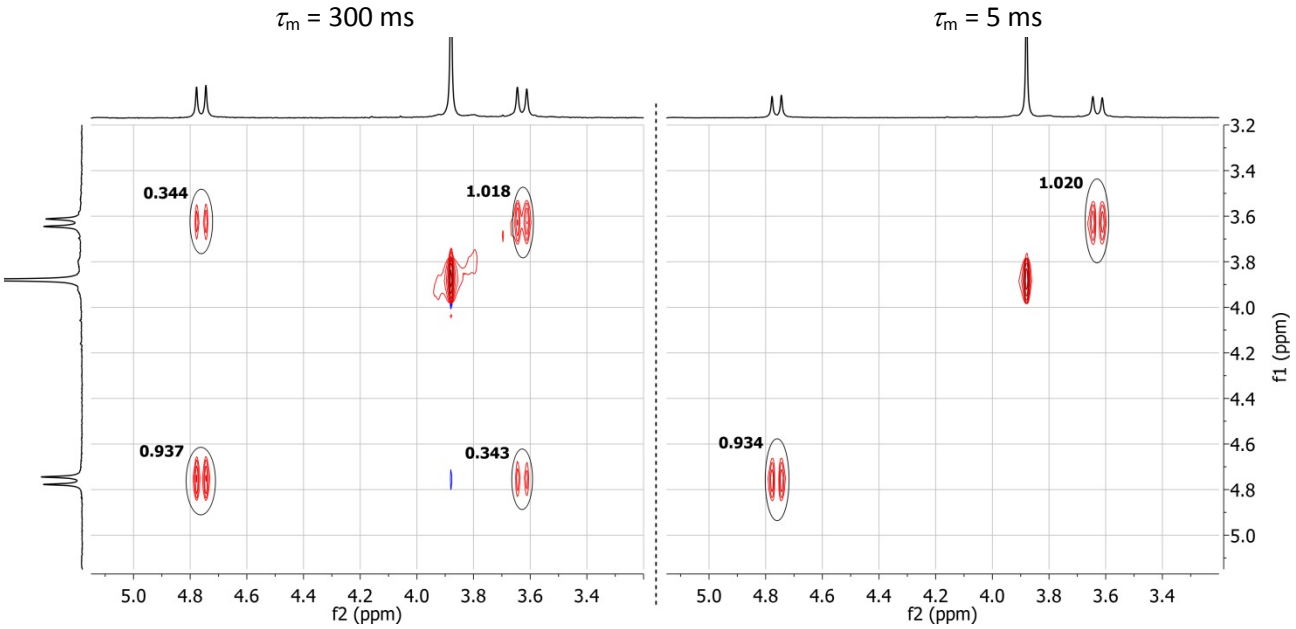

^{1}H 2D EXSY (400 MHz), $CDCl_3$, 272.5 K

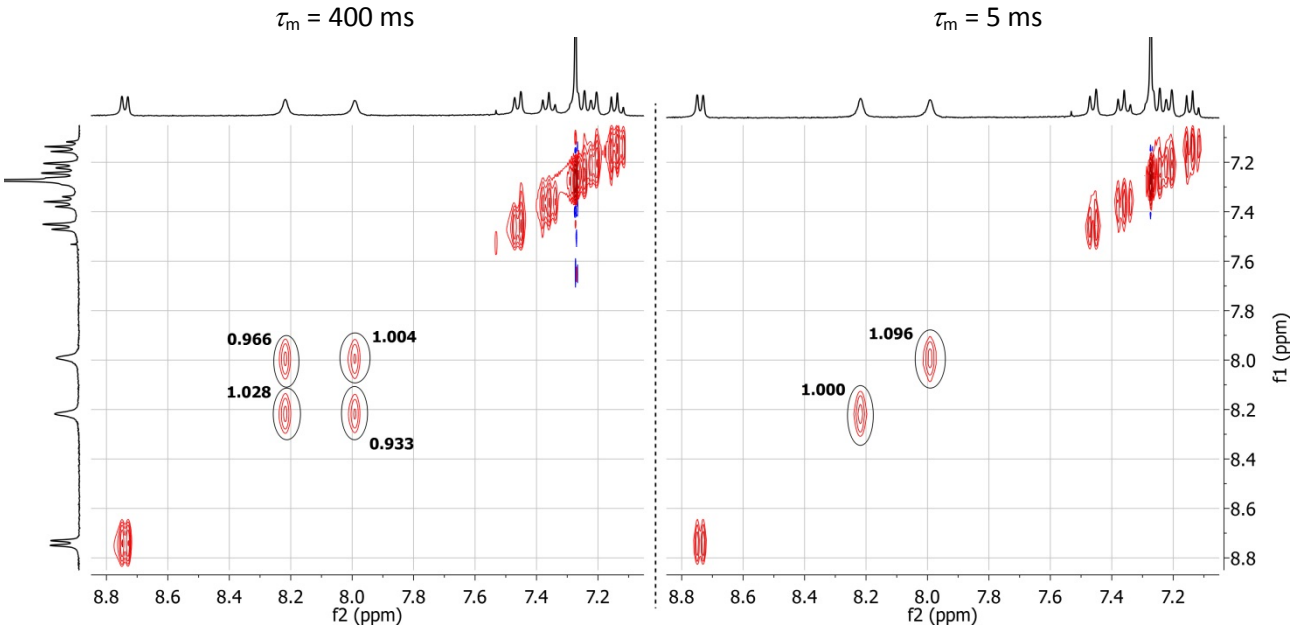

Figure S6. ^{1}H 2D EXSY spectra acquired to calculate the cone inversion (top) and panel rotation (bottom) exchange barriers of **1a** in $CDCl_3$ ([**1a**] = 2.0 mM).

Table S1. Integral values (*I*) and the resulting rate constants in $CDCl_3$ obtained with EXSYCalc.

	I		I_{ref}	τ_m ms	T K	k_1 s^{-1}	k_{-1} s^{-1}	k_{mean} s^{-1}	$\Delta G^{\ddagger}$ kcal·mol^{-1}
Cone flip	1.018	0.343	1.020	300	299.3	1.170	1.282	1.226	17.4±0.2[a]
	0.344	0.937	0.934						
Panel rotation	1.004	0.933	1.096	400	272.5	4.369	4.143	4.256	15.1±0.2[a]
	0.966	1.028	1.000						

[a] The errors are estimated by calculating the extreme $\Delta G^{\ddagger}$ values obtained with a 5% error bias in integration.

^{1}H 2D EXSY (400 MHz), CD_2Cl_2, 299.4 K

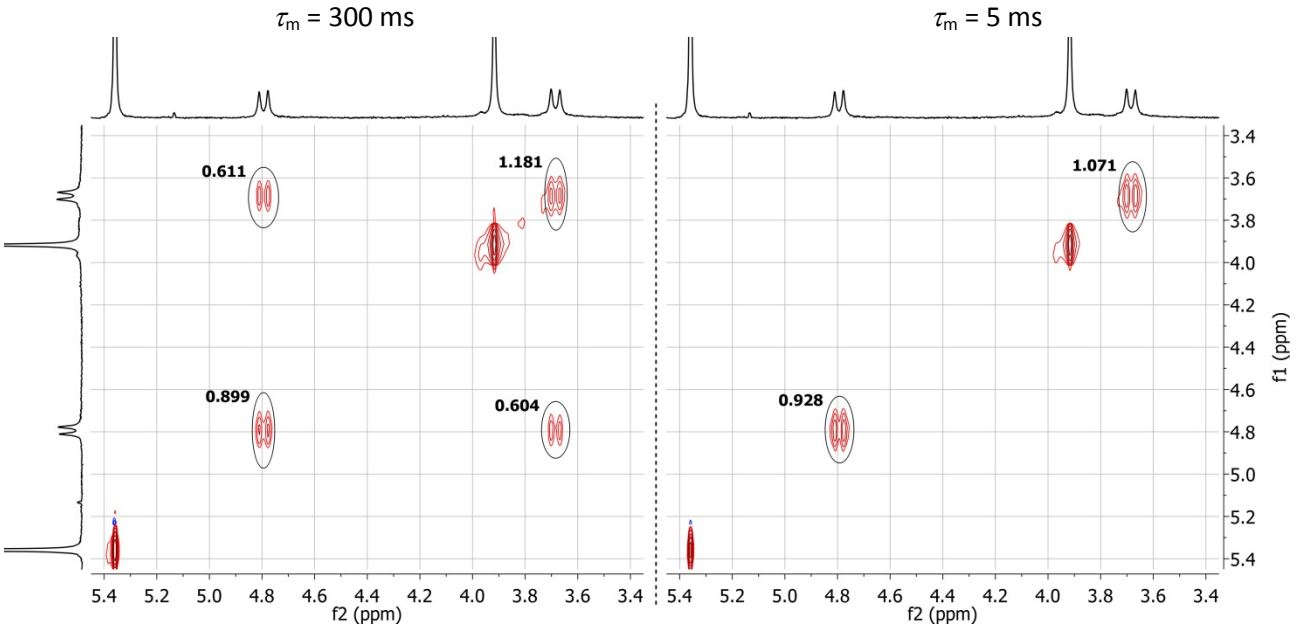

^{1}H 2D EXSY (400 MHz), CD_2Cl_2, 250.9 K

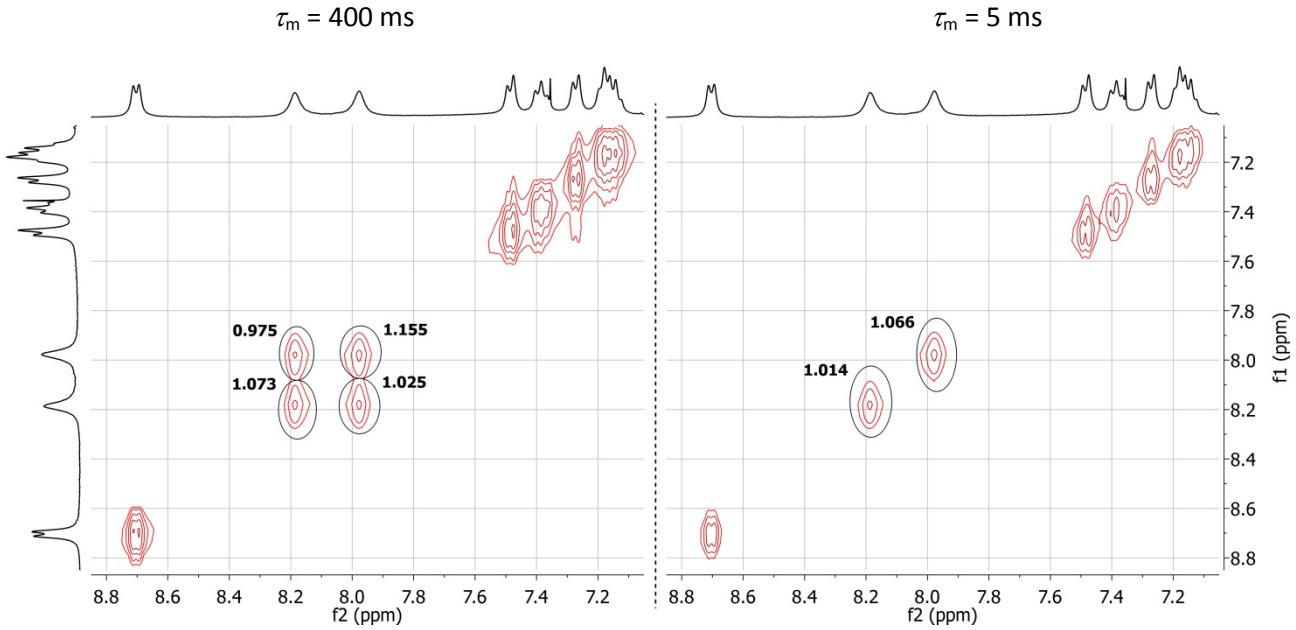

Figure S7. ^{1}H 2D EXSY spectra acquired to calculate the cone inversion (top) and panel rotation (bottom) exchange barriers of **1a** in CD_2Cl_2 ([**1a**] = 2.0 mM).

Table S2. Integral values (*I*) and the resulting rate constants in CD_2Cl_2 obtained with EXSYCalc.

	I		***I*** $_{ref}$	τ_m ms	**T K**	k_1 **s^{-1}**	k_{-1} **s^{-1}**	k_{mean} **s^{-1}**	**ΔG‡ kcal·mol^{-1}**
Cone flip	1.181	0.611	1.071	300	299.4	2.111	2.409	2.260	17.0±0.2[a]
	0.604	0.899	0.928						
Panel rotation	1.155	1.025	1.066	400	250.9	3.654	3.654	3.654	13.9±0.2[a]
	0.975	1.073	1.014						

[a] The errors are estimated by calculating the extreme ΔG‡ values obtained with a 5% error bias in integration.

3.2 Lineshape analysis

Lineshape analysis of the coalescence experiments for H_c/H_d ($CDCl_3$) was carried out with iNMR v6.2.2 (Mestrelab Research). The first order rate constant for the exchange k was determined at each temperature by lineshape fitting. Then, ln(k/t) was plotted against 1/T and a linear regression was obtained in order to extract the activation parameters ($\Delta H^{\ddagger}$, $\Delta S^{\ddagger}$) from the Eyring equation in logarithmic form (2). The errors for the activation barriers ($\Delta G^{\ddagger}$) are expressed as the root mean square deviation between the $\Delta G^{\ddagger}$ values obtained from the calculated activation parameters and the ones calculated from the measured rate constant *k* at each temperature. It is worth noting that the small contribution of the entropic component to the total $\Delta G^{\ddagger}$ value facilitates the comparison of barriers obtained by EXSY experiments at different temperatures.

$$\ln\left(\frac{k}{T}\right) = -\frac{\Delta H^{\ddagger}}{R}\frac{1}{T} + \left(\frac{k_B}{h}\right) + \frac{\Delta S^{\ddagger}}{R} \qquad (2)$$

Calculated activation parameters: $\Delta H^{\ddagger} = 58.2\ kJ \cdot mol^{-1} = 13.9\ kcal \cdot mol^{-1}$

$\Delta S^{\ddagger} = 15.5\ J \cdot K^{-1} \cdot mol^{-1} = -3.7\ cal \cdot K^{-1} \cdot mol^{-1}$

Activation barriers for panel flip: $\Delta G^{\ddagger}_{272.5} = 14.9 \pm 0.3\ kcal \cdot mol^{-1}$

$\Delta G^{\ddagger}_{299.3} = 15.0 \pm 0.3\ kcal \cdot mol^{-1}$

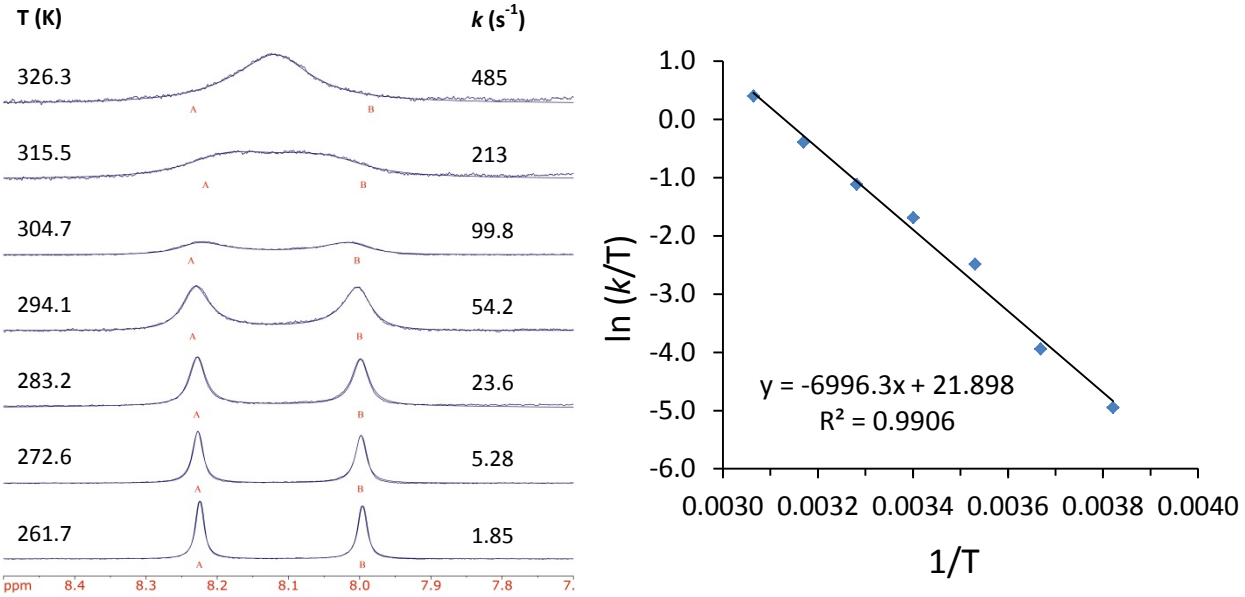

Figure S8. Stack of ^{1}H NMR spectra showing the coalescence for protons H_c/H_d with overlapping simulated spectra and the resulting rate constants *k*. The corresponding plot of ln(*k*/T) vs 1/T is shown on the right.

4 Structures of guests G1-G9.

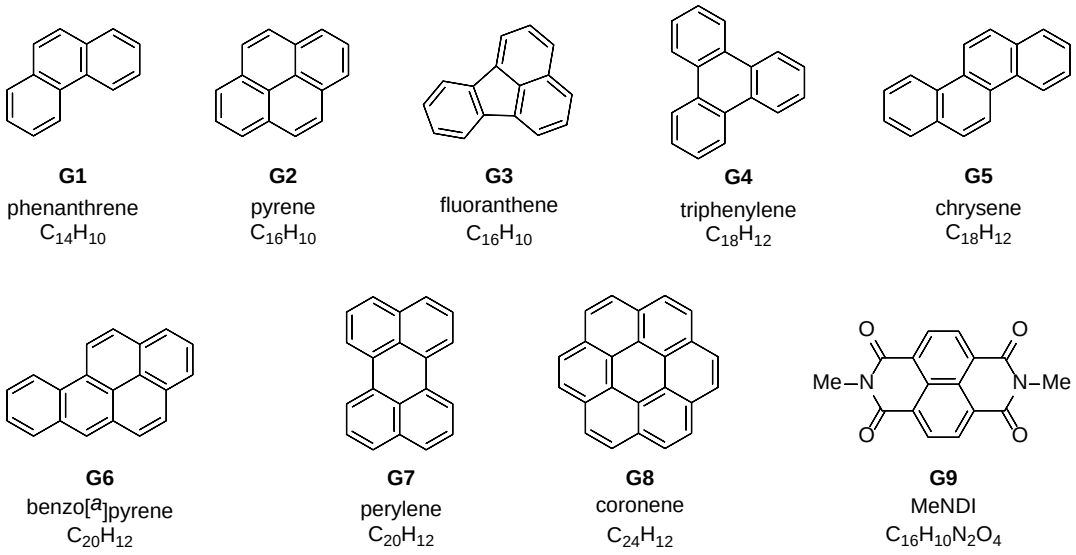

Figure S9. Structures of guests employed in this study. PAHs are ordered in increasing molecular weight.

5 ^{1}H NMR titrations with 1a.

All titrations have been repeated three times. The K_a values are reported as the mean value of the replicates, and the error expressed as the confidence interval at 95% confidence, based on the standard deviation of the three experiments.

5.1 Coronene (G8)

In $CDCl_3$

Owing to the low solubility of coronene in chloroform, a reverse titration was performed. A 2.1 mM stock solution of **G8** in CD_2Cl_2 was prepared (solution **A**). A 10.0 mM solution of **1a** in **A** was then prepared (solution **B**). A 0.400 mL initial volume of solution **A** was titrated with increasing amounts of solution **B**. A ^{1}H NMR spectrum was recorded after each addition. After referencing each spectrum, the δ values for the coronene resonance were extracted and fit to a binding isotherm using Bindfit.[6,7]

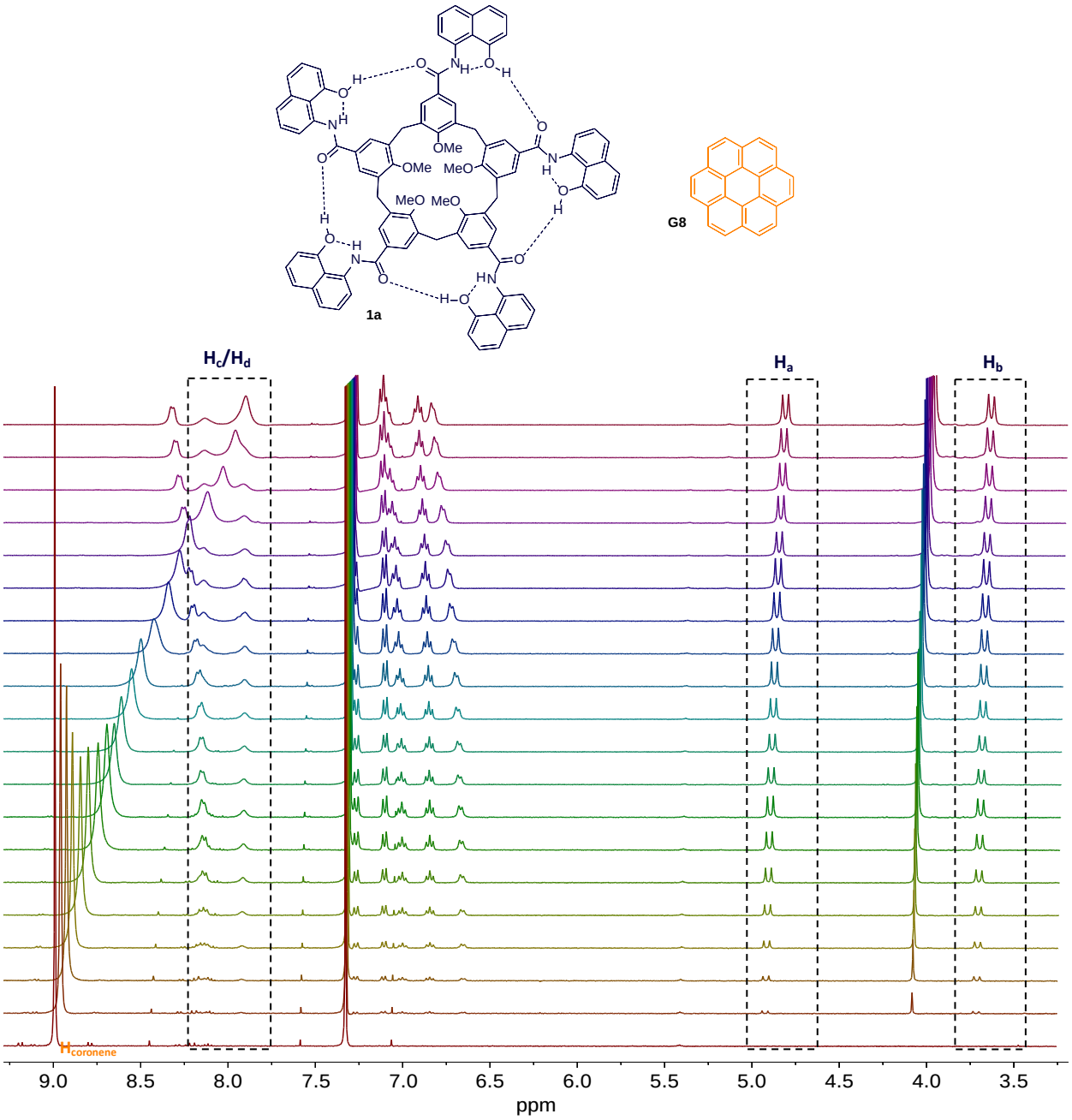

Figure S10. ^{1}H NMR titration of **G8** with **1a** in $CDCl_3$. The regions of resonances H_a/H_b and H_c/H_d are highlighted, showing that **1a** retains its dynamic features throughout the titration.

K_a	**362±4 M^{-1}**
RMS	7.2x10^{-3}
Covariance	2.7x10^{-4}

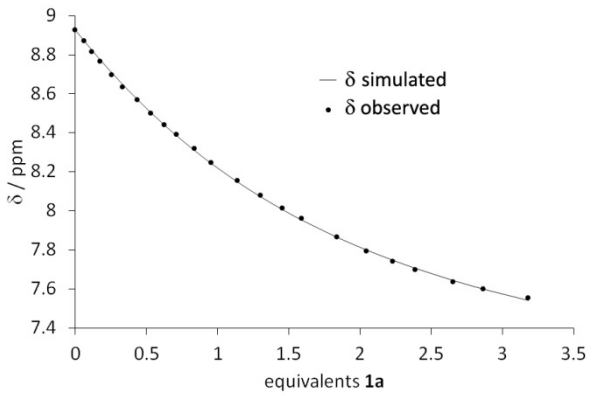

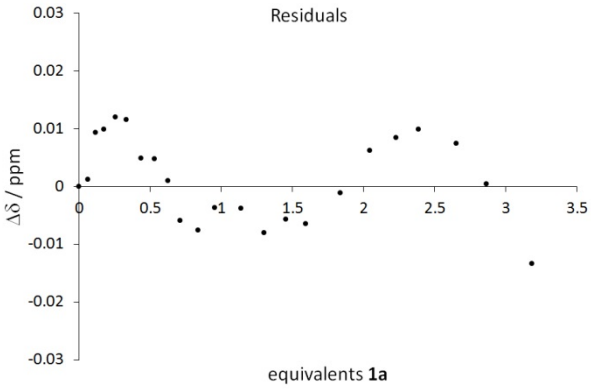

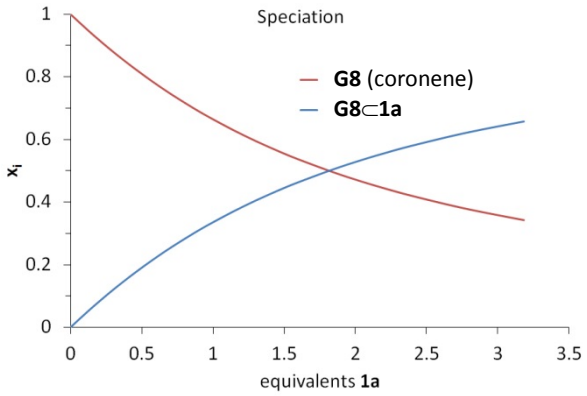

In CD_2Cl_2

Owing to the low solubility of coronene in dichloromethane, a reverse titration was performed. A 2.0 mM stock solution of **G8** in CD_2Cl_2 was prepared (solution **A**). A 10.1 mM solution of **1a** in **A** was then prepared (solution **B**). A 0.400 mL initial volume of solution **A** was titrated with increasing amounts of solution **B**. A ^{1}H NMR spectrum was recorded after each addition. After referencing each spectrum, the δ values for the coronene resonance were extracted and fit to a binding isotherm using Bindfit.[6,7]

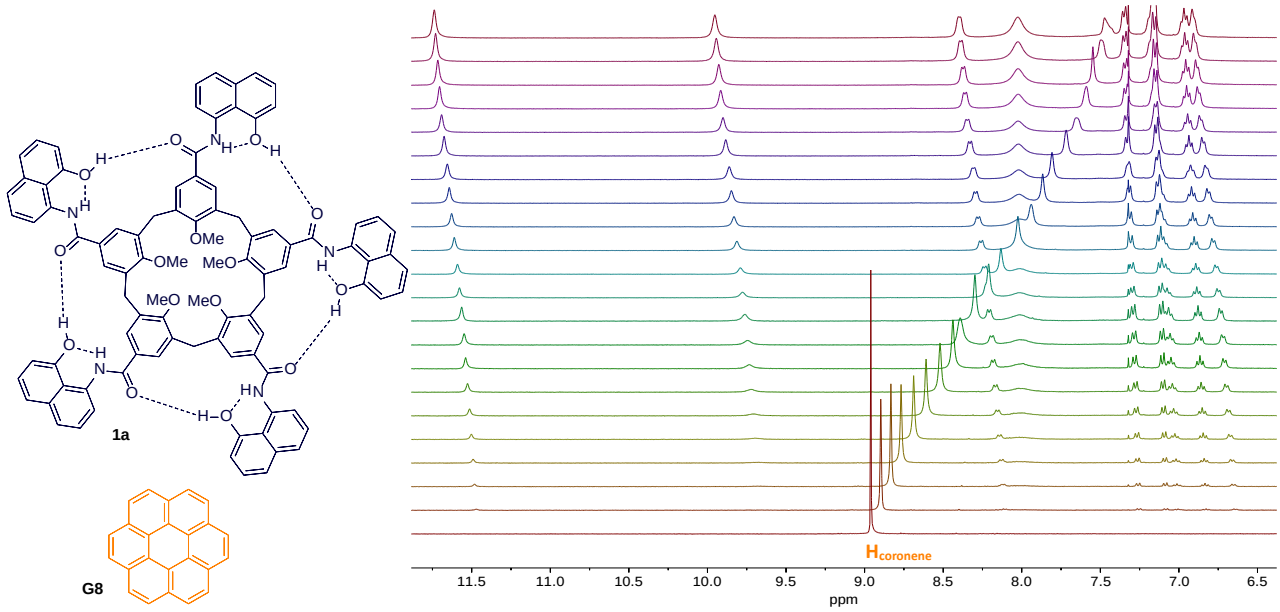

Figure S11. ^{1}H NMR titration of **G8** with **1a** in CD_2Cl_2.

K_a	**444±5 M^{-1}**
RMS	8.0×10^{-3}
Covariance	2.7×10^{-4}

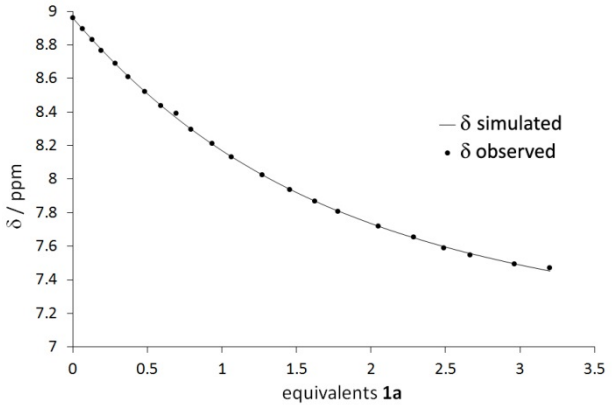

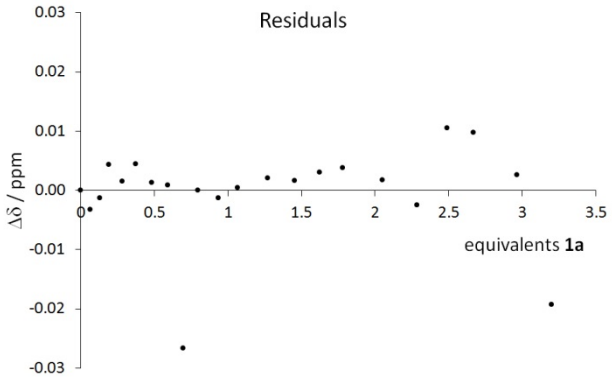

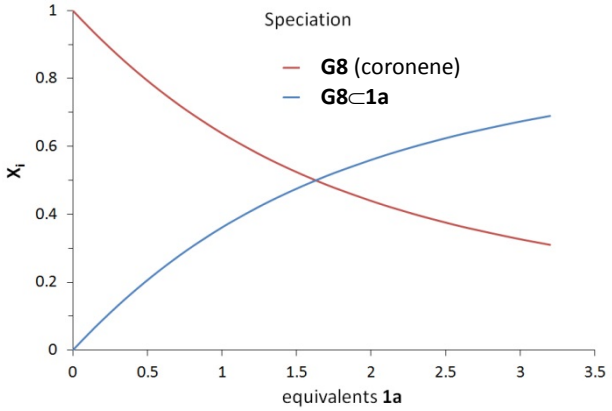

5.2 *N,N*-Dimethyl-naphthalenediimide (MeNDI, G9)

In $CDCl_3$

A 2.0 mM stock solution of **1a** in $CDCl_3$ was prepared (solution **A**). A 10.2 mM solution of **G9** in **A** was then prepared (solution **B**). A 0.400 mL initial volume of solution **A** was titrated with increasing amounts of solution **B**. A ^{1}H NMR spectrum was recorded after each addition. After referencing each spectrum, the δ values for the indicated resonances of **1a** were extracted and fit to a binding isotherm using Bindfit.[6]

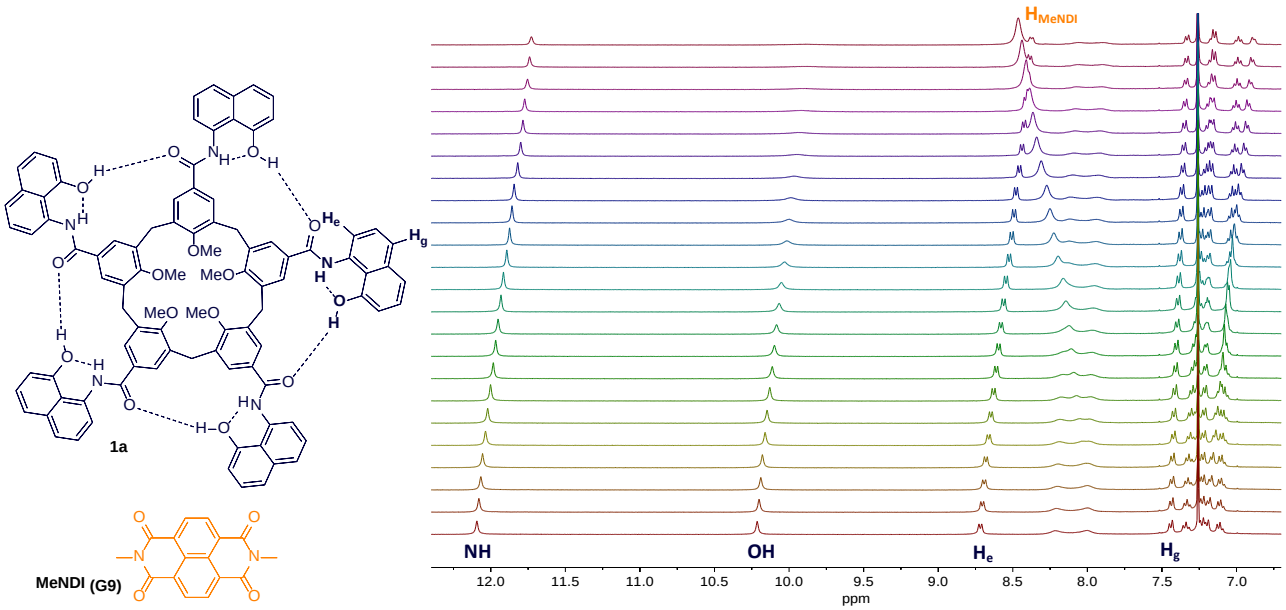

Figure S12. ^{1}H NMR titration of **1a** with **G9** in $CDCl_3$.

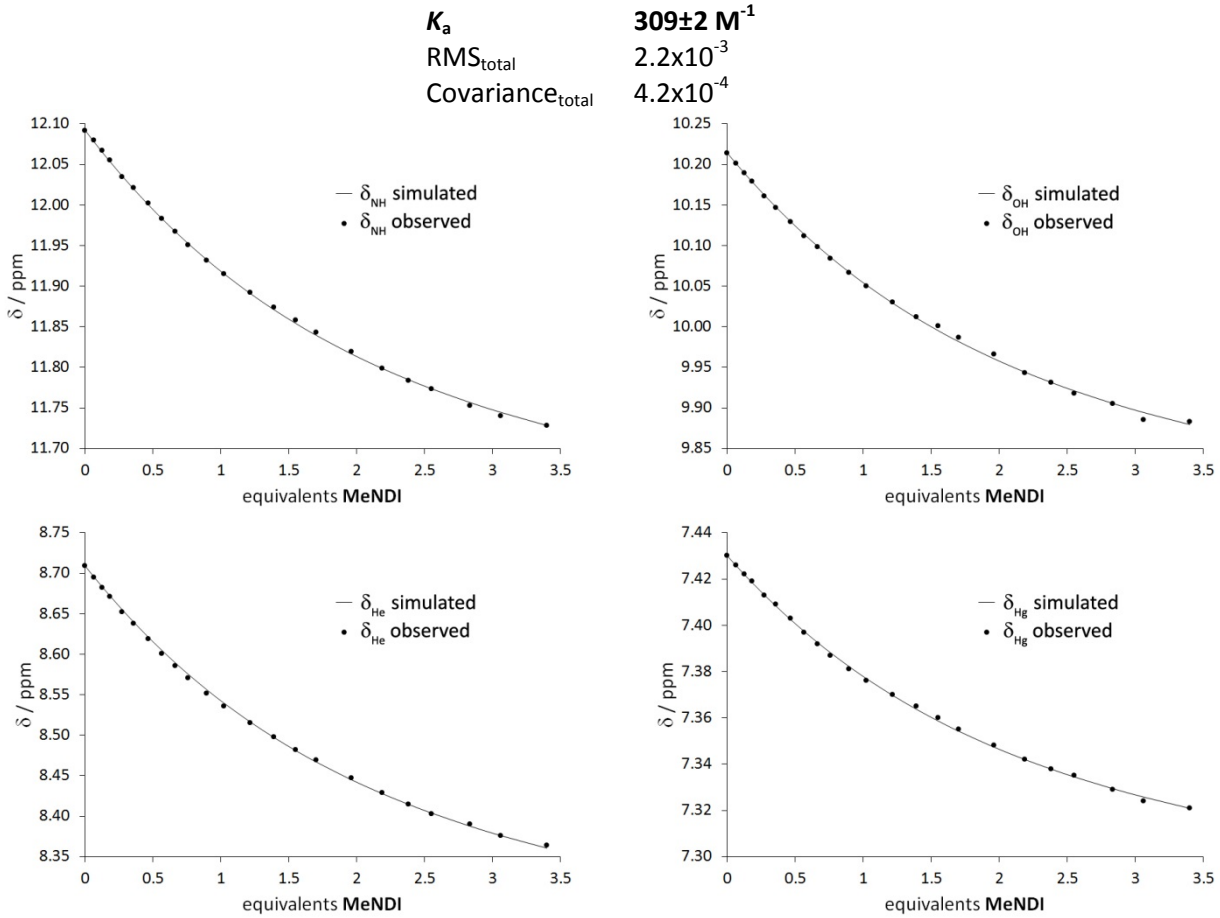

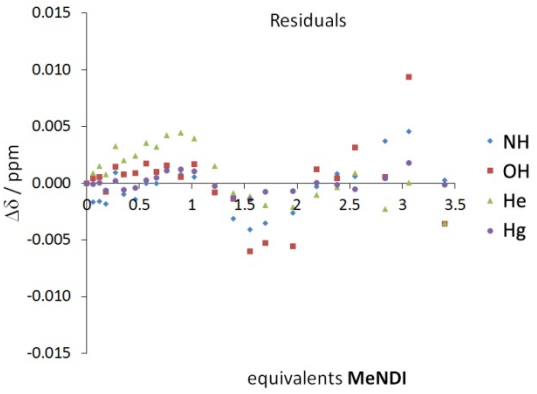

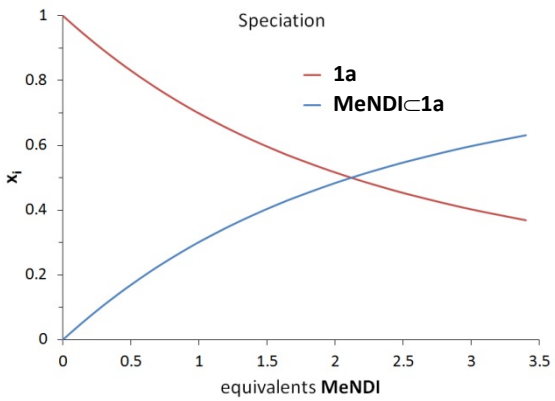

In CD_2Cl_2

A 2.1 mM stock solution of **1a** in CD_2Cl_2 was prepared (solution **A**). A 9.9 mM solution of **G9** in **A** was then prepared (solution **B**). A 0.400 mL initial volume of solution **A** was titrated with increasing amounts of solution **B**. A ^{1}H NMR spectrum was recorded after each addition. After referencing each spectrum, the δ values for the indicated resonances of **1a** were extracted and fit to a binding isotherm using Bindfit.[6]

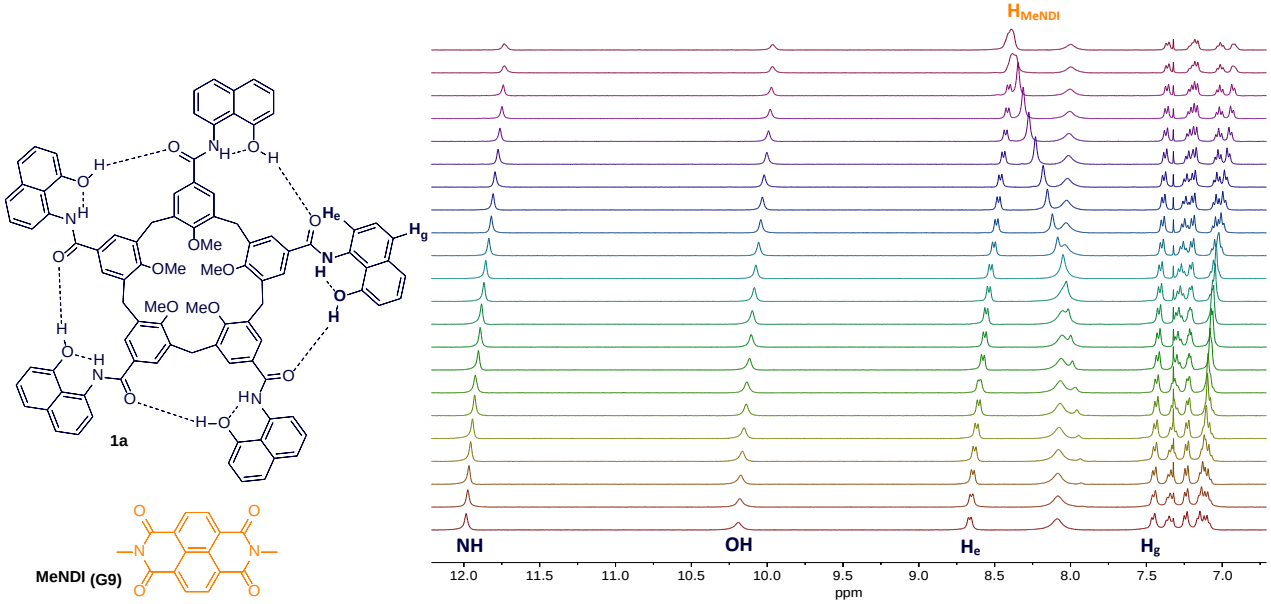

Figure S13. ^{1}H NMR titration of **1a** with **G9** in CD_2Cl_2.

K_a	**299±3 M^{-1}**
RMS$_{total}$	2.9x10^{-3}
Covariance$_{total}$	1.3x10^{-3}

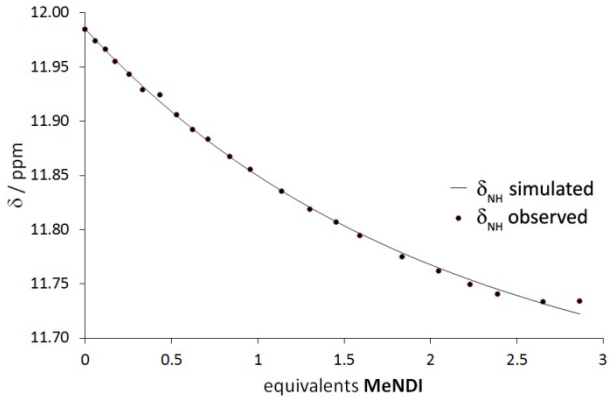

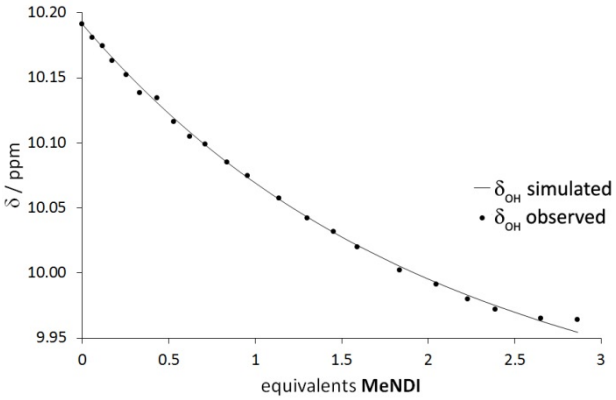

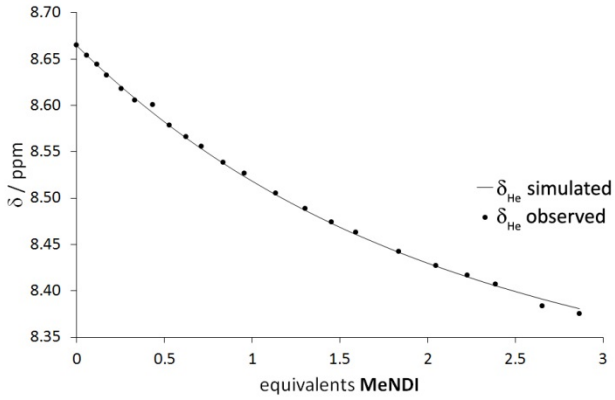

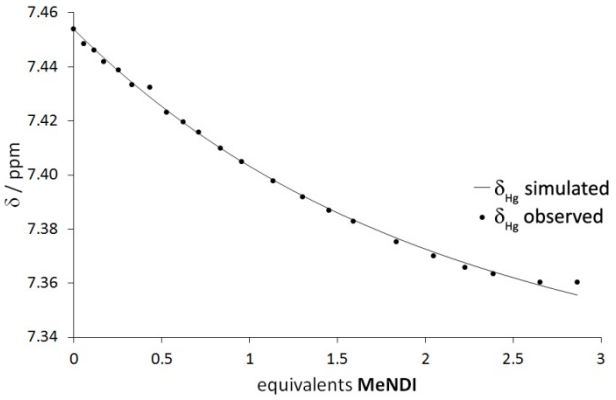

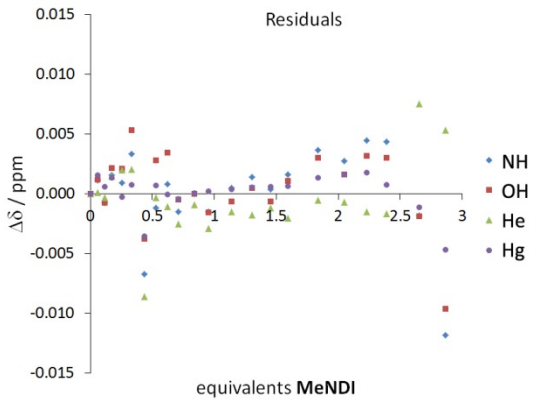

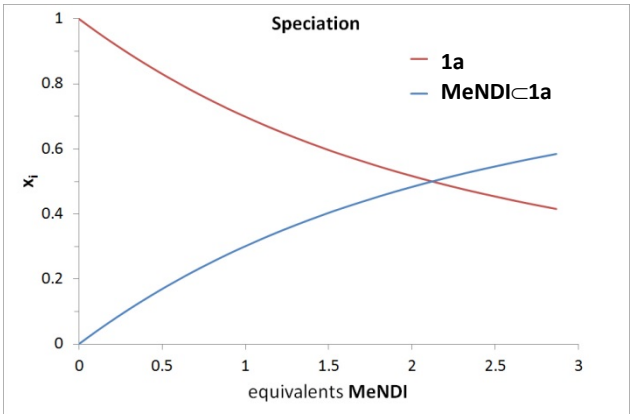

6 HRMS and MS/MS of complex G8⊂1a

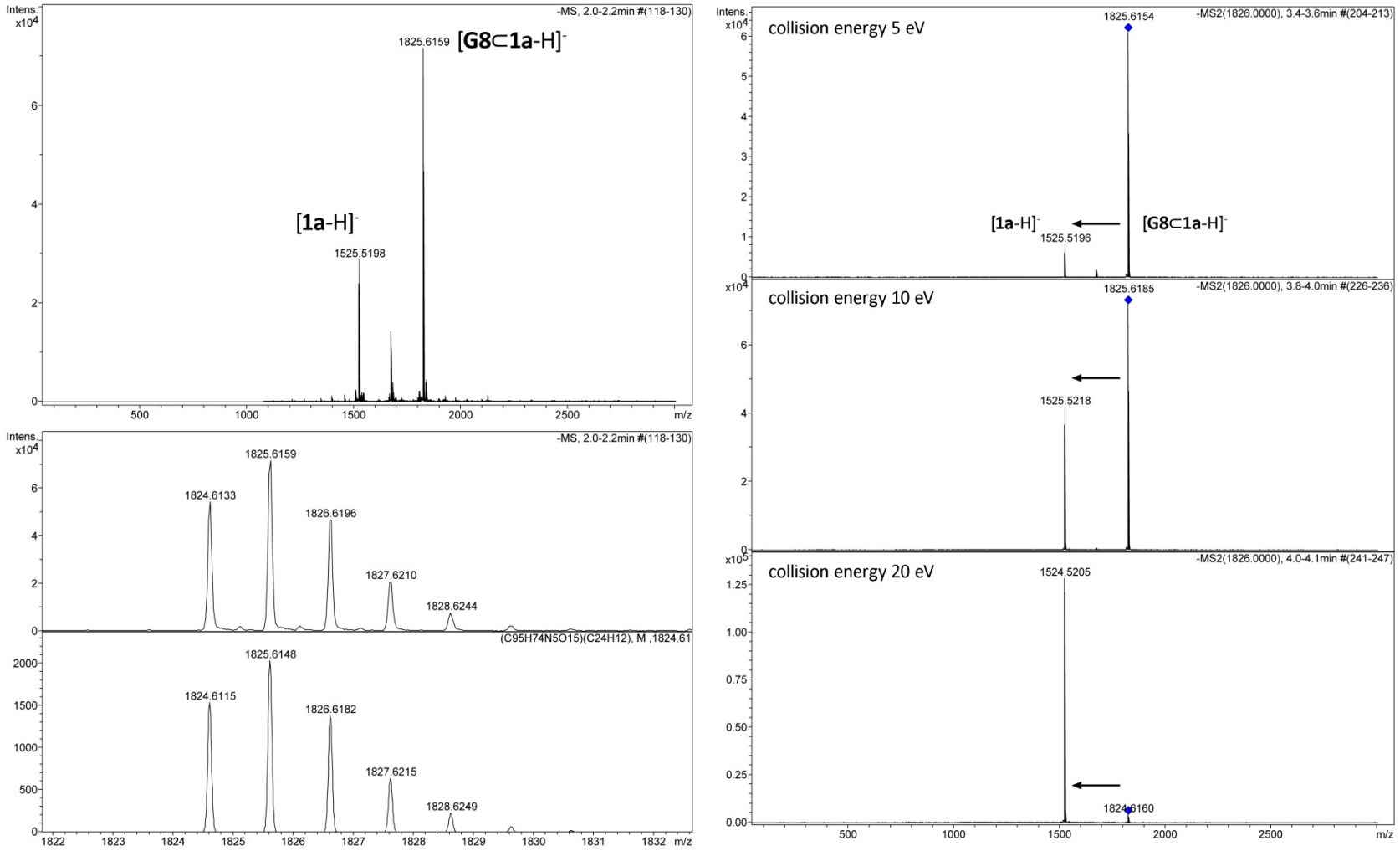

Fig S14. Right: ESI(-) HRMS of complex **G8⊂1a**. The 1:1 complex is the most abundant species. Lesser amounts of free cavitand (**1a**) and higher aggregates (**1a**)$_2$·**G8**, (**1a**)$_2$·(**G8**)$_2$ are also observed. Left: ESI(-) MS/MS spectrum of fragment [**G8⊂1a**-H]$^-$ at increasing collision energies, showing displacement of coronene (**G8**) from the cavity.

7 Molecular modelling studies

Starting models for **1a**, 3$CHCl_3$⊂**1a**, **G7**⊂**1a**, **G8**⊂**1a**, and **G9**⊂**1a** were constructed with the GUI of Spartan '18 v1.2.0 and optimized at the PM6 semiempirical level with the same program, except for 3$CHCl_3$⊂**1a**, which was minimized by molecular mechanics (MMFF). These models were used as starting geometries for DFT calculations and molecular dynamics (MD) simulations.

7.1 DFT Calculations

Geometries of the minima for **1a**, **G7**⊂**1a,** and **G8**⊂**1a** in the gas phase were optimized without symmetry constraints with the Gaussian 16 program[8] using the DFT B3LYP hybrid exchange-correlation functional,[9] the 6-31G(d) basis set,[10] and taking into account dispersion effects with the DFT-D3BJ correction by Grimme.[11] After geometry optimization, frequency calculations were done to ensure that the obtained minima have only real frequencies.

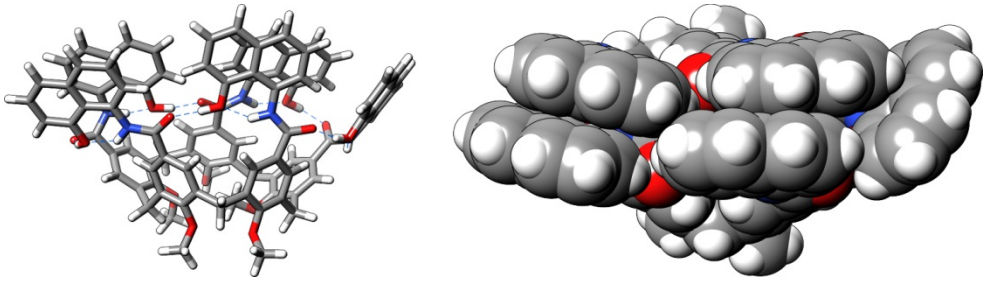

Figure S15. DFT-minimized structure of free host **1a**.

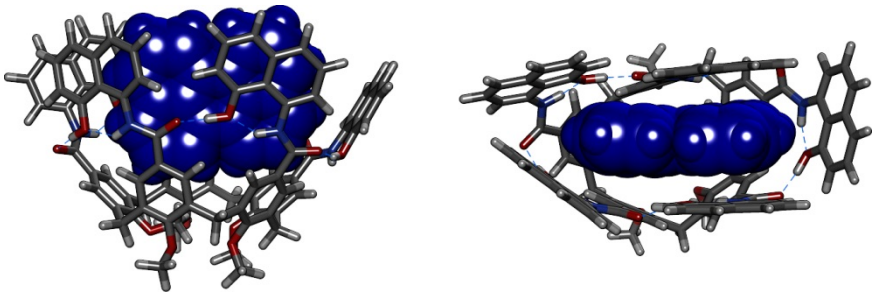

Figure S16. DFT-minimized structure of complex **G7**⊂**1a**.

Geometries of the stationary points are available from the ioChem-BD (www.iochem-bd.org) structure repository through the following link:

https://iochem.udg.edu:8443/browse/review-collection/100/760/9046b720581bb298e0288870

7.2 MD Simulations

The parameters for the cavitand (**1a**) and the guests (**G8**, **G9**) for the MD simulations were generated within the Antechamber module of Amber 16 using the generalized Amber force field (GAFF),[12] with partial charges calculated according to AM1-BCC scheme[13] using Antechamber. Each system was immersed in a pre-equilibrated truncated cubic box of chloroform molecules with an internal offset distance of 10 Å, using the Amber 16 Leap module. All calculations were done using the GAFF force field. A two-stage geometry optimization approach was performed. First, a short minimization of the chloroform molecules positions, with positional restraints on solute by a harmonic potential with a force constant of 500 kcal mol^{-1} $Å^{-2}$ was done. The second stage was an unrestrained minimization of all the atoms in the simulation cell. Then, the systems were heated using six 50 ps steps, incrementing the temperature 50 K each step (0-300 K) under

constant-volume, periodic-boundary conditions and the particle-mesh Ewald approach[14] to introduce long-range electrostatic effects. For these steps, a 10 Å cut-off was applied to Lennard-Jones and electrostatic interactions. Bonds involving hydrogen were constrained with the SHAKE algorithm. Harmonic restraints of 10 kcal mol^{-1} were applied to the solute, and the Langevin equilibration scheme was used to control and equalize the temperature. The time step was kept at 2 fs during the heating stages, allowing potential inhomogeneities to self-adjust. Each system was then equilibrated for 2 ns with a 2 fs time step at a constant pressure of 1 atm (NPT ensemble). Then MD simulations were performed under the NVT ensemble (constant volume) and periodic-boundary conditions. For free **1a**, 1000 ns (1 μs) of MD simulation were computed, whereas 500 ns MDs were obtained for the **G7⊂1a**, **G8⊂1a** and **G9⊂1a** ensembles. The MD trajectories were obtained with the CPPTRAJ module of AMBER 16. Video files of the trajectories are provided as supplementary files. For **G7** only the fragment showing guest departure is provided (260 – 270 ns).

8 References

(1) Wang, L.; Barth, C. W.; Sibrian-Vazquez, M.; Escobedo, J. O.; Lowry, M.; Muschler, J.; Li, H.; Gibbs, S. L.; Strongin, R. M., *ACS Omega* **2017,** *2* (1), 154-163.

(2) (a) Garcia-Hartjes, J.; Bernardi, S.; Weijers, C. A. G. M.; Wennekes, T.; Gilbert, M.; Sansone, F.; Casnati, A.; Zuilhof, H., *Org. Biomol. Chem.* **2013,** *11* (26), 4340-4349. (b) Pasquale, S.; Sattin, S.; Escudero-Adán, E. C.; Martínez-Belmonte, M.; de Mendoza, J., *Nat Commun* **2012,** *3*, 785. (c) Stewart, D. R.; Gutsche, C. D., *Org. Prep. Proced. Int.* **1993,** *25* (1), 137-139. (d) Coruzzi, M.; Andreetti, G. D.; Bocchi, V.; Pochini, A.; Ungaro, R., *J. Chem. Soc., Perkin Trans. 2* **1982,** (9), 1133-1138.

(3) Vreekamp, R. H.; Verboom, W.; Reinhoudt, D. N., *J. Org. Chem.* **1996,** *61* (13), 4282-4288.

(4) (a) Perrin, C. L.; Dwyer, T. J., *Chem. Rev.* **1990,** *90* (6), 935-967. (b) Meier, B. H.; Ernst, R. R., *J. Am. Chem. Soc.* **1979,** *101* (21), 6441-6442. (c) Jeener, J.; Meier, B. H.; Bachmann, P.; Ernst, R. R., *J. Chem. Phys.* **1979,** *71* (11), 4546-4553.

(5) https://mestrelab.com/software/freeware/
http://nmr-analysis.blogspot.com/2008/11/exsycalc-free-software-for-nmr-analysis.html

(6) Brynn Hibbert, D.; Thordarson, P., C*hem. Commun. 2***016,** 5*2* (87), 12792-12805.

(7) http://app.supramolecular.org/bindfit/

(8) Frisch, M. J.; Trucks, G. W.; Schlegel, H. B.; Scuseria, G. E.; Robb, M. A.; Cheeseman, J. R.; Scalmani, G.; Barone, V.; Petersson, G. A.; Nakatsuji, H.; Li, X.; Caricato, M.; Marenich, A. V.; Bloino, J.; Janesko, B. G.; Gomperts, R.; Mennucci, B.; Hratchian, H. P.; Ortiz, J. V.; Izmaylov, A. F.; Sonnenberg, J. L.; Williams; Ding, F.; Lipparini, F.; Egidi, F.; Goings, J.; Peng, B.; Petrone, A.; Henderson, T.; Ranasinghe, D.; Zakrzewski, V. G.; Gao, J.; Rega, N.; Zheng, G.; Liang, W.; Hada, M.; Ehara, M.; Toyota, K.; Fukuda, R.; Hasegawa, J.; Ishida, M.; Nakajima, T.; Honda, Y.; Kitao, O.; Nakai, H.; Vreven, T.; Throssell, K.; Montgomery Jr., J. A.; Peralta, J. E.; Ogliaro, F.; Bearpark, M. J.; Heyd, J. J.; Brothers, E. N.; Kudin, K. N.; Staroverov, V. N.; Keith, T. A.; Kobayashi, R.; Normand, J.; Raghavachari, K.; Rendell, A. P.; Burant, J. C.; Iyengar, S. S.; Tomasi, J.; Cossi, M.; Millam, J. M.; Klene, M.; Adamo, C.; Cammi, R.; Ochterski, J. W.; Martin, R. L.; Morokuma, K.; Farkas, O.; Foresman, J. B.; Fox, D. J. G*aussian 16,* Wallingford, CT, 2016.

(9) (a) Stephens, P. J.; Devlin, F. J.; Chabalowski, C. F.; Frisch, M. J., T*he Journal of Physical Chemistry 1***994,** 9*8* (45), 11623-11627. (b) Becke, A. D., J*. Chem. Phys. 1***993,** 9*8* (7), 5648-5652. (c) Lee, C.; Yang, W.; Parr, R. G., P*hysical Review B 1***988,** 3*7* (2), 785-789.

(10) (a) Rassolov, V. A.; Pople, J. A.; Ratner, M. A.; Windus, T. L., J*. Chem. Phys. 1***998,** 1*09* (4), 1223-1229. (b) Hariharan, P. C.; Pople, J. A., T*heoretica chimica acta 1***973,** 2*8* (3), 213-222.

(11) (a) Grimme, S.; Ehrlich, S.; Goerigk, L., J*. Comput. Chem. 2***011,** 3*2* (7), 1456-1465. (b) Grimme, S.; Antony, J.; Ehrlich, S.; Krieg, H., J*. Chem. Phys. 2***010,** 1*32* (15), 154104.

(12) Wang, J.; Wolf, R. M.; Caldwell, J. W.; Kollman, P. A.; Case, D. A., J*. Comput. Chem. 2***004,** 2*5* (9), 1157-1174.

(13) Jakalian, A.; Bush, B. L.; Jack, D. B.; Bayly, C. I., J*. Comput. Chem. 2***000,** 2*1* (2), 132-146.

(14) Darden, T.; York, D.; Pedersen, L., J*. Chem. Phys. 1***993,** 9*8* (12), 10089-10092.

9 NMR Spectra of new compounds

^{1}H NMR (400 MHz, $CDCl_3$, 273K)

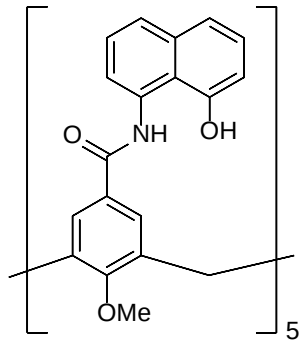

1a

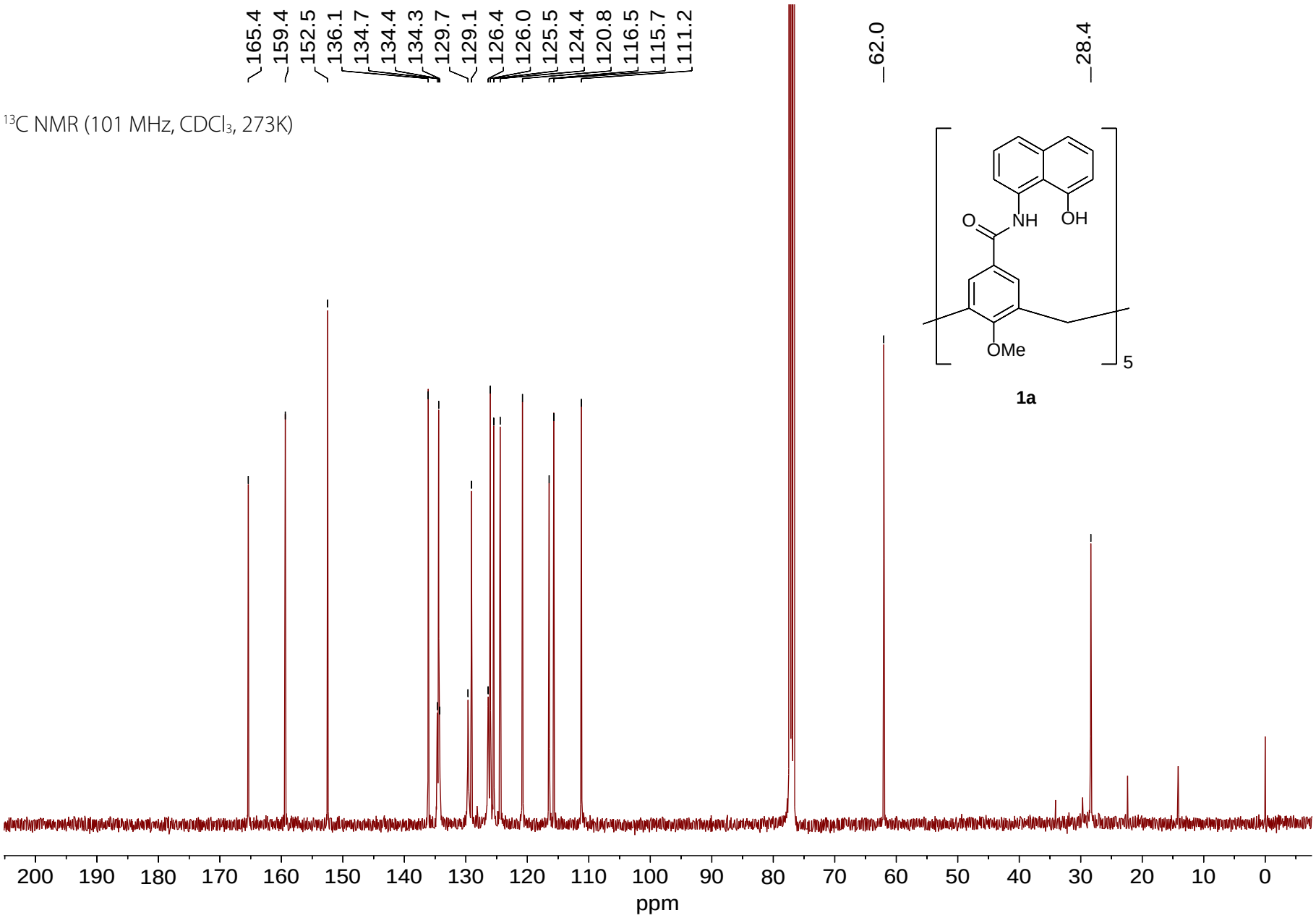

^{13}C NMR (101 MHz, $CDCl_3$, 273K)

1a

^{1}H - ^{13}C HSQC NMR (400 MHz, $CDCl_3$, 273K)

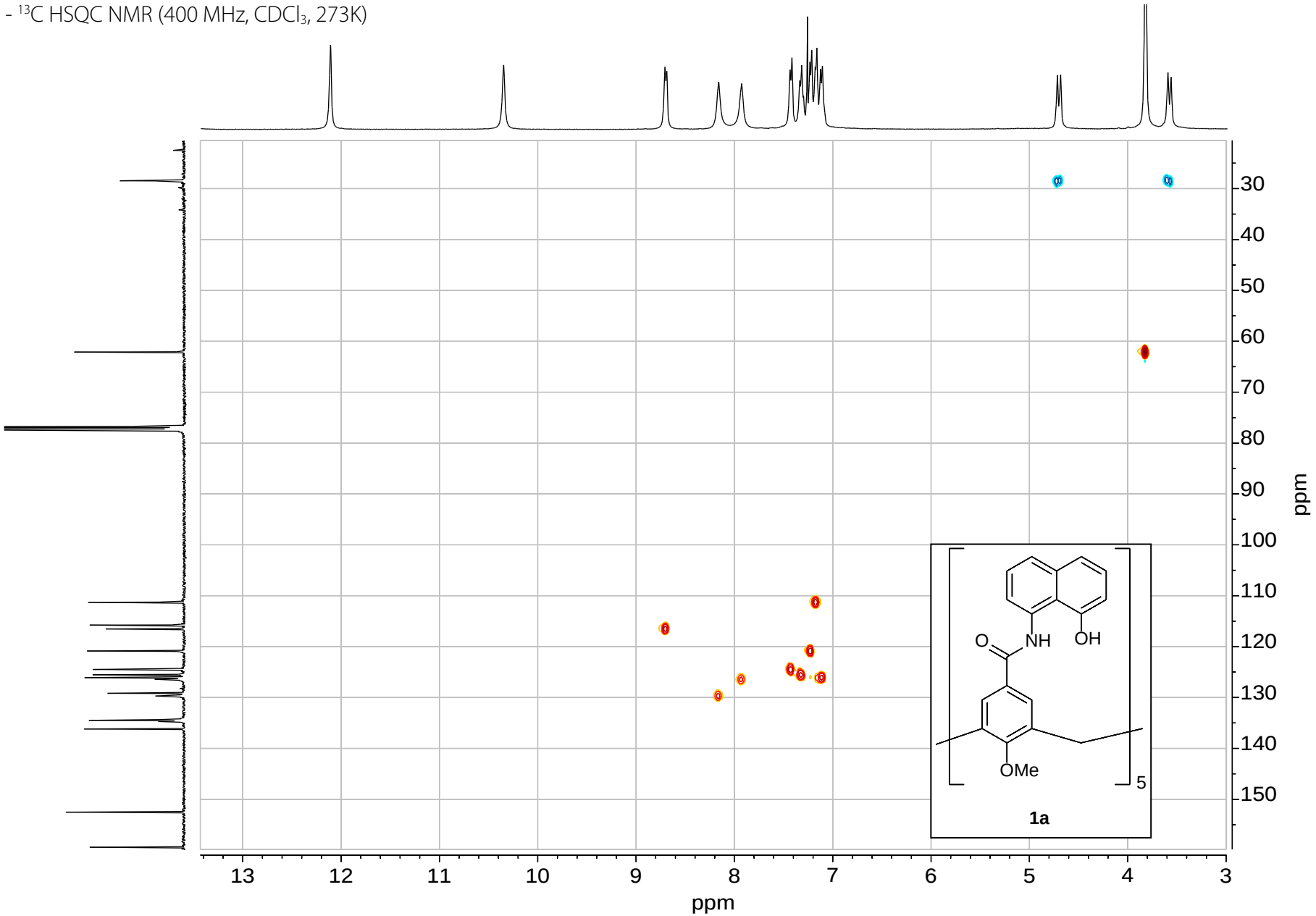

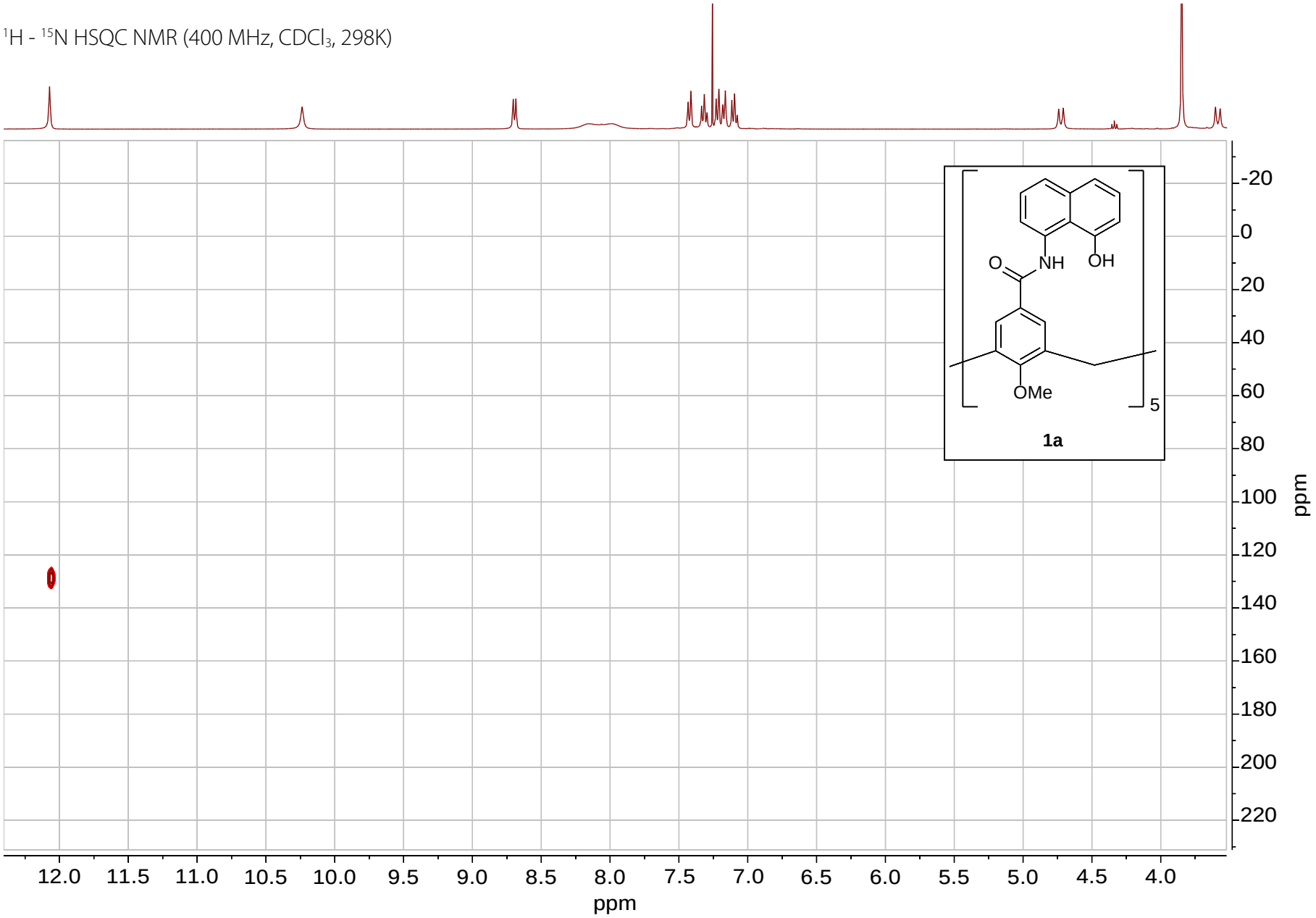
^{1}H - ^{15}N HSQC NMR (400 MHz, $CDCl_3$, 298K)
O
NH
OH
OMe
5
1a
-20
0
20
40
60
80
100
120
140
160
180
200
220
ppm
12.0
11.5
11.0
10.5
10.0
9.5
9.0
8.5
8.0
7.5
7.0
6.5
6.0
5.5
5.0
4.5
4.0
ppm

^{1}H 2D ROESY (400 MHz), $CDCl_3$

299.3 K, τ_m = 300 ms

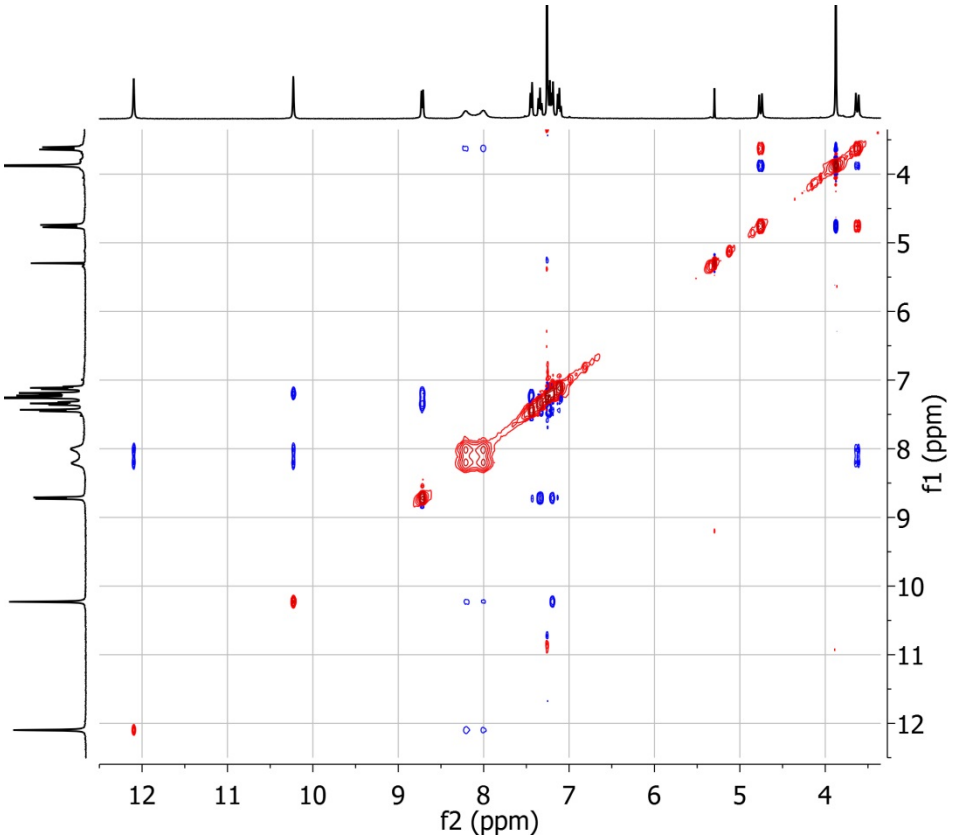

261.7 K, τ_m = 300 ms

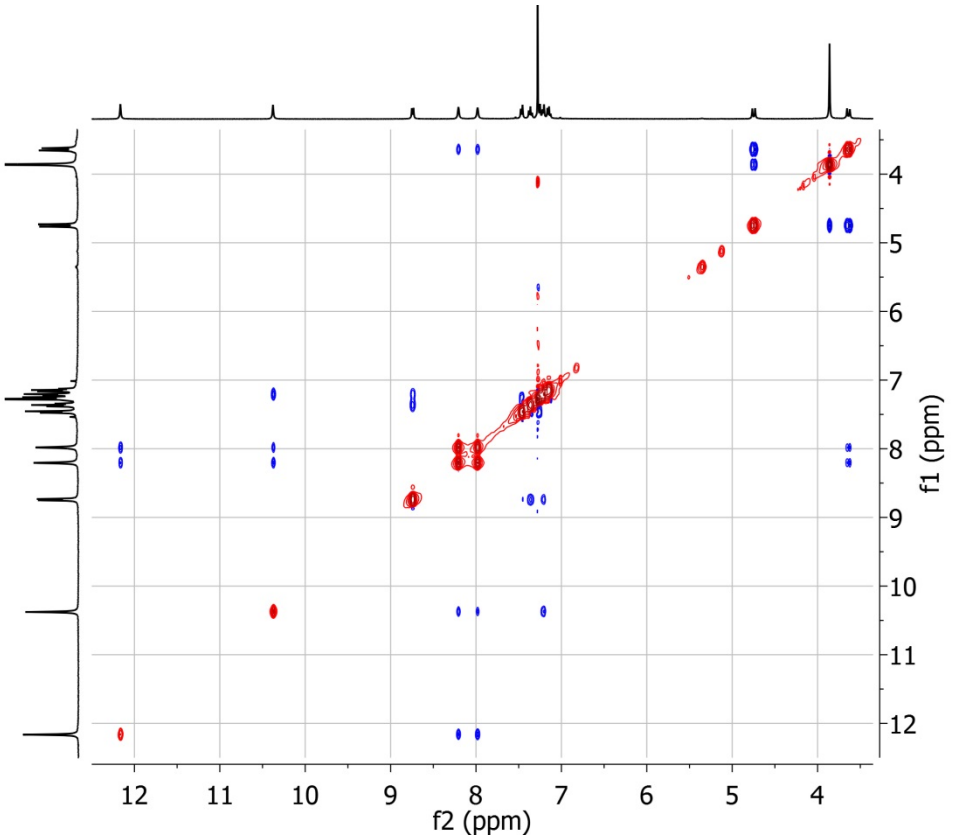

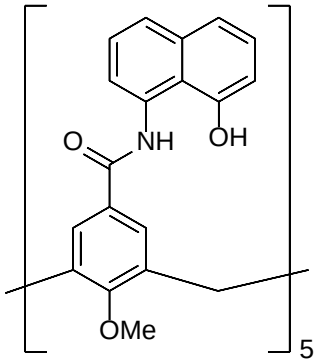

1a

^{1}H NMR (400 MHz, $CDCl_3$, 298K)

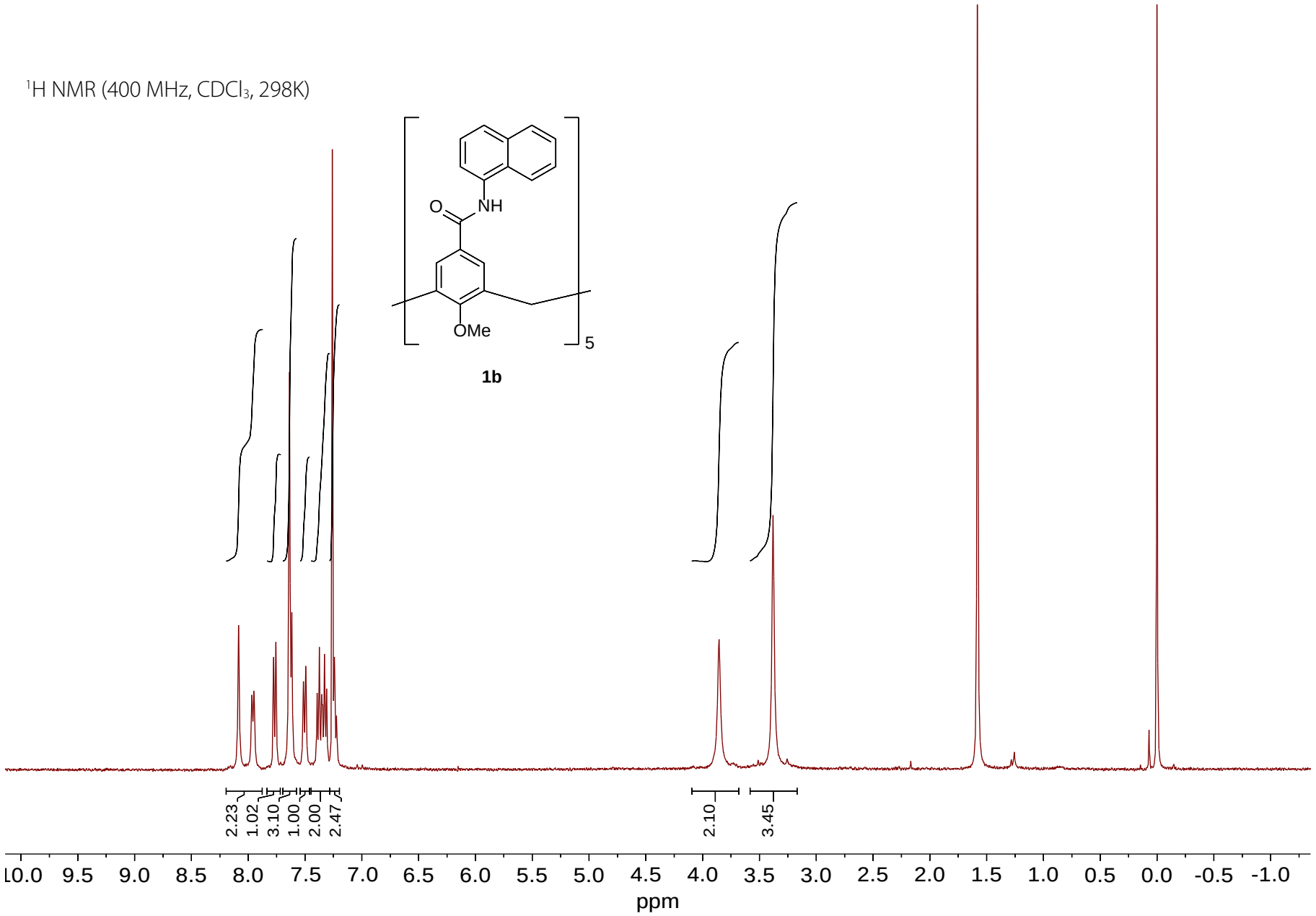

1b

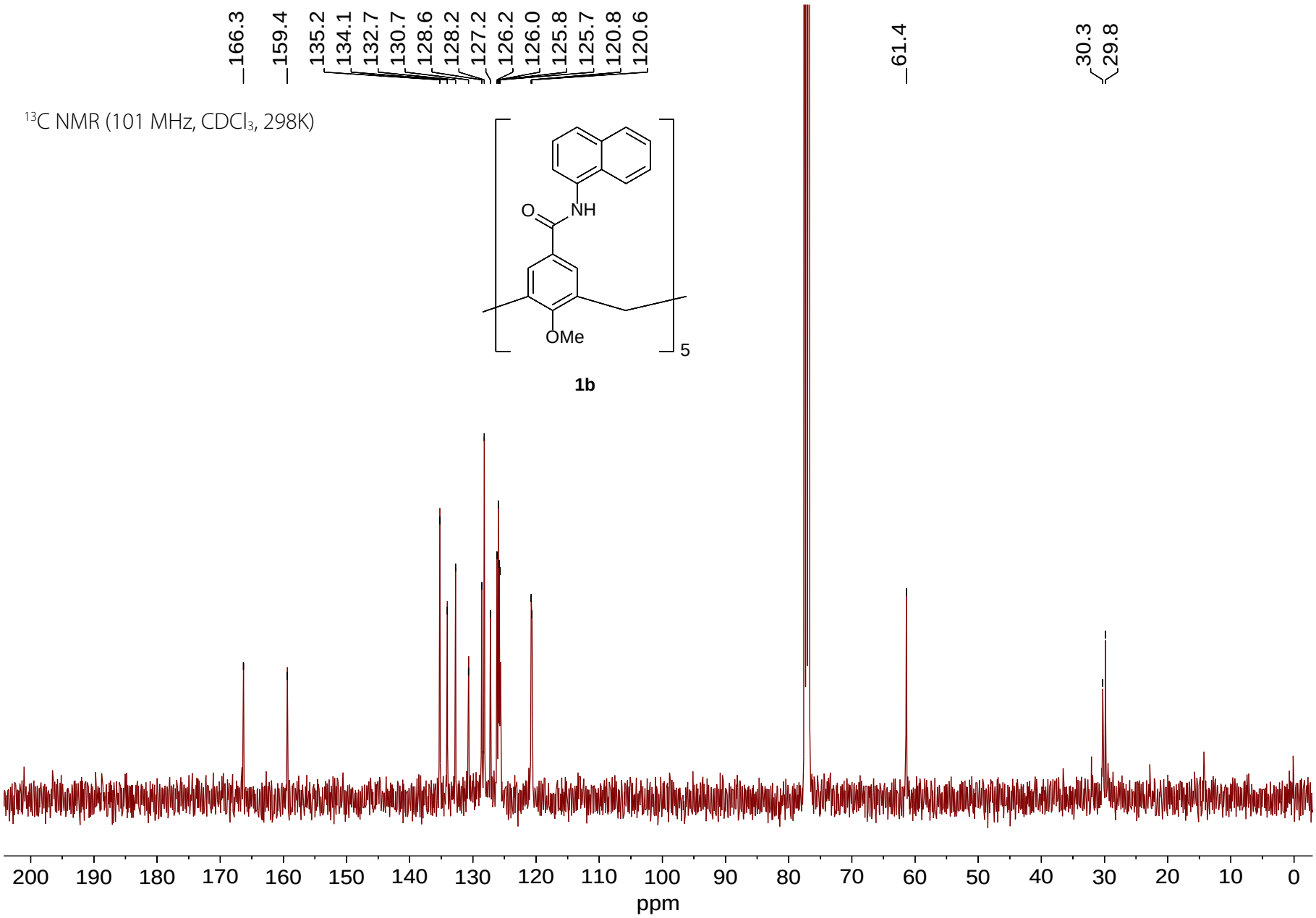
166.3
159.4
135.2
134.1
132.7
130.7
128.6
128.2
127.2
126.2
126.0
125.8
125.7
120.8
120.6
61.4
30.3
29.8
13C NMR (101 MHz, CDCl3, 298K)
O
NH
OMe
5
1b
200
190
180
170
160
150
140
130
120
110
100
90
80
70
60
50
40
30
20
10
0
ppm

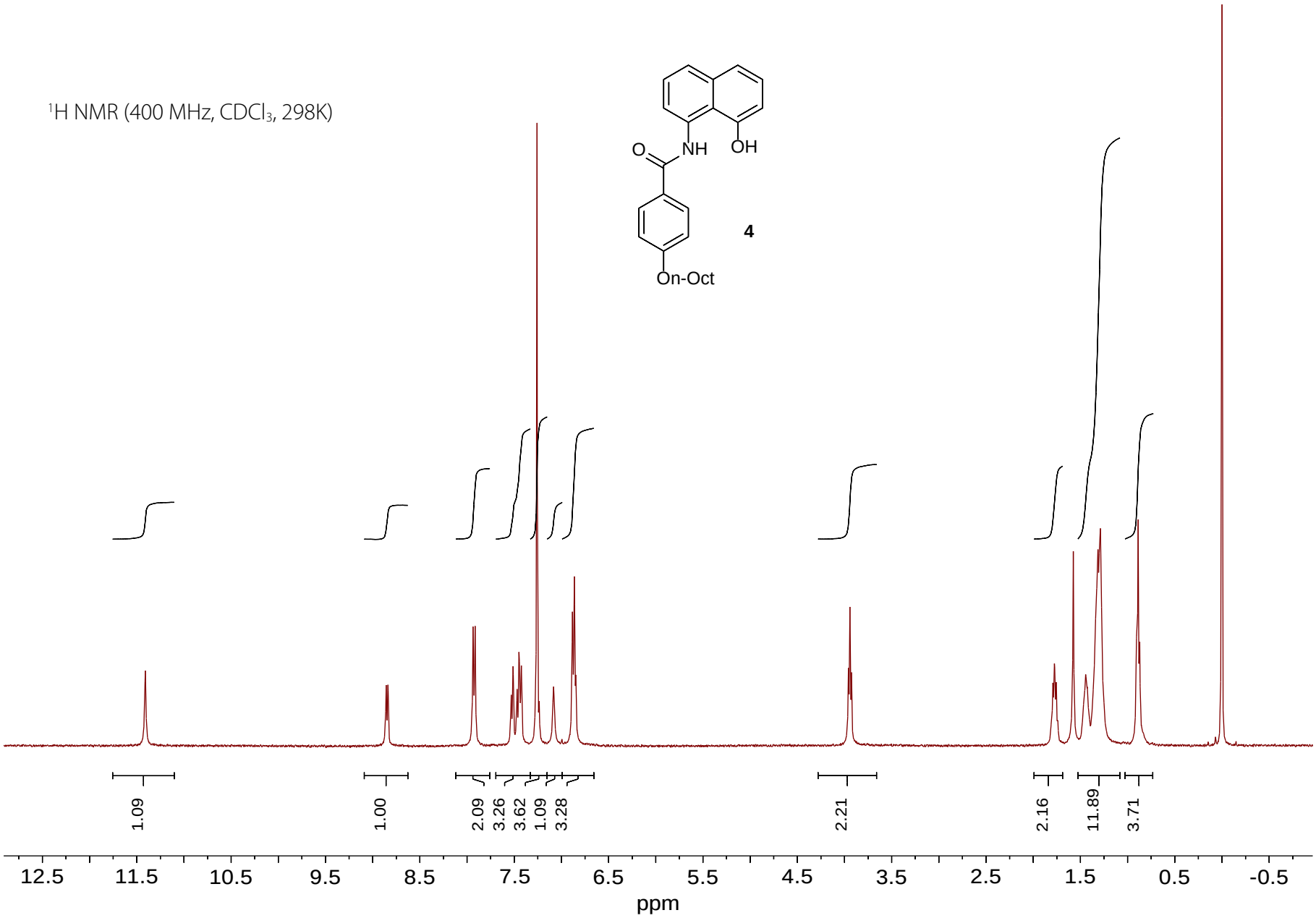
^{1}H NMR (400 MHz, $CDCl_3$, 298K)
O
NH
OH
On-Oct
4
1.09
1.00
2.09
3.26
3.62
1.09
3.28
2.21
2.16
11.89
3.71
12.5
11.5
10.5
9.5
8.5
7.5
6.5
5.5
4.5
3.5
2.5
1.5
0.5
-0.5
ppm

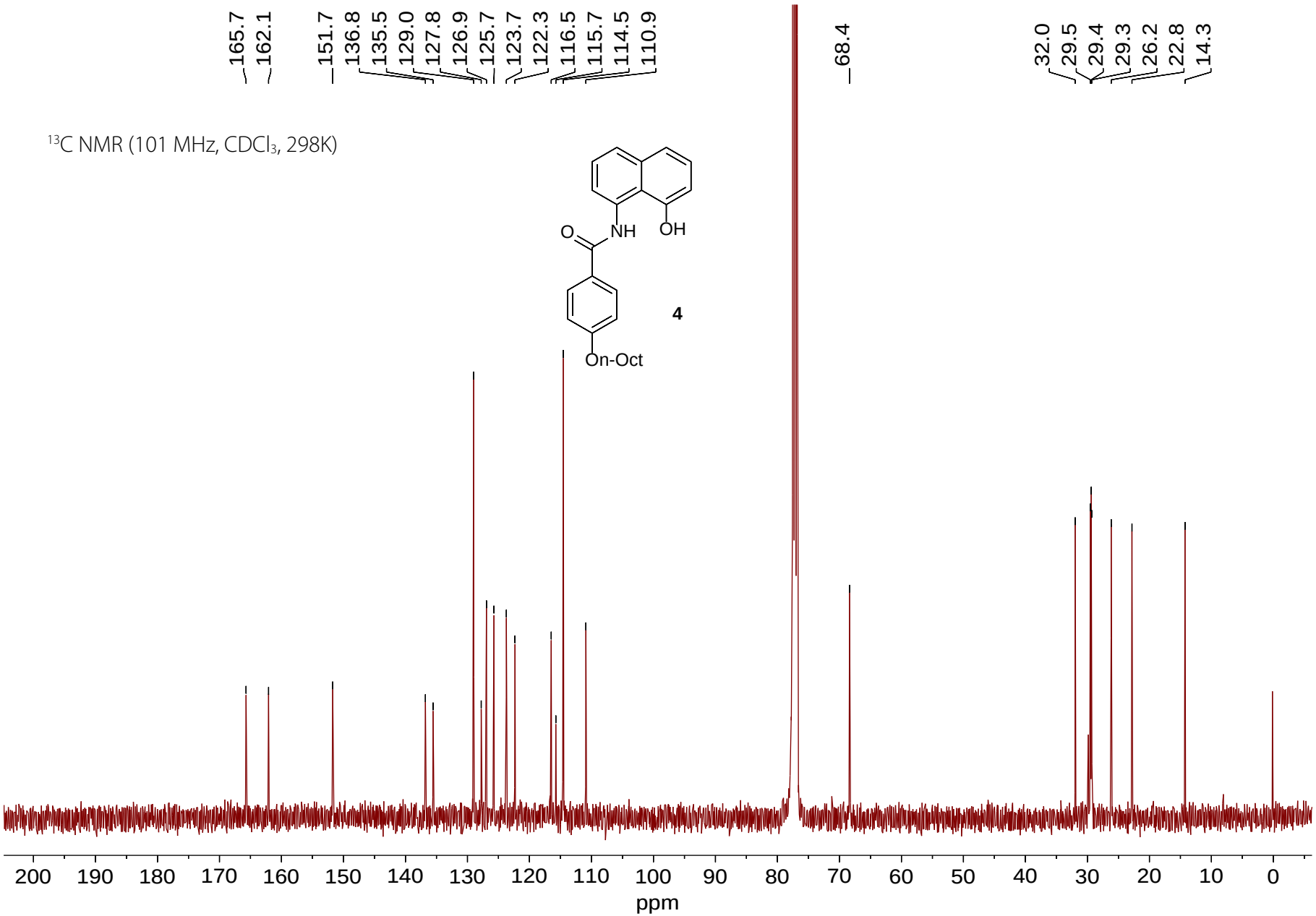
165.7
162.1
151.7
136.8
135.5
129.0
127.8
126.9
125.7
123.7
122.3
116.5
115.7
114.5
110.9
68.4
32.0
29.5
29.4
29.3
26.2
22.8
14.3
13C NMR (101 MHz, CDCl3, 298K)
O
NH
OH
On-Oct
4
200
190
180
170
160
150
140
130
120
110
100
90
80
70
60
50
40
30
20
10
0
ppm

10 HRMS spectra of new compounds

Generic Display Report

Analysis Info

Analysis Name	D:\Data\Agustí Lledó\20171127_000012.d	Acquisition Date	11/27/2017 3:53:48 PM
Method	tune_high_negative.m	Operator	Univ. Girona
Sample Name	DLM035 (1884)	Instrument	micrOTOF-Q II
Comment			

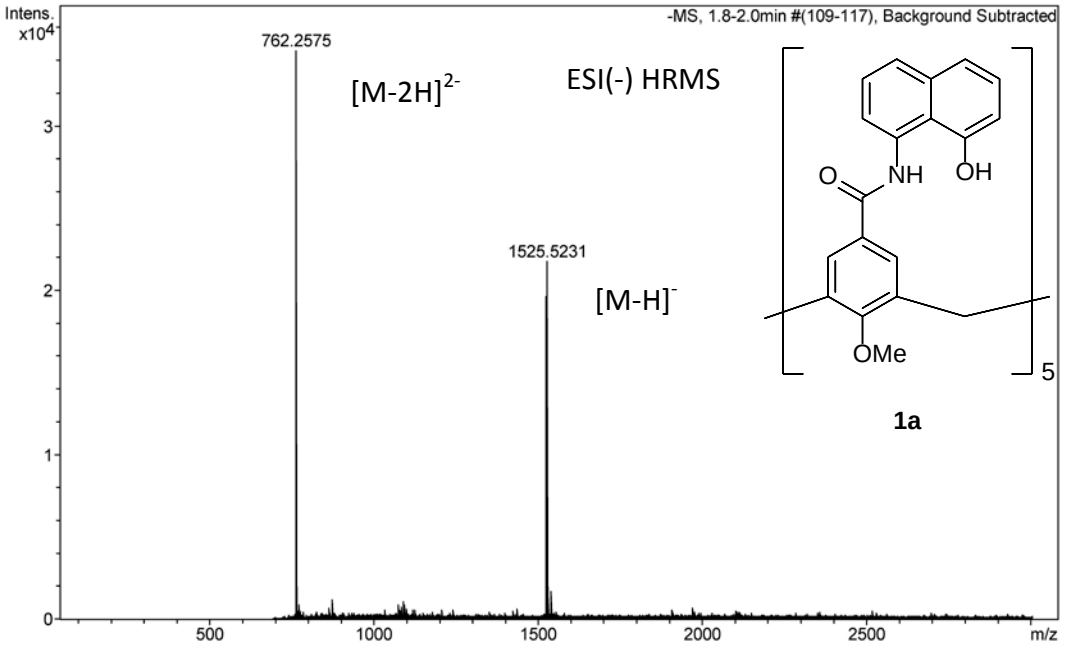

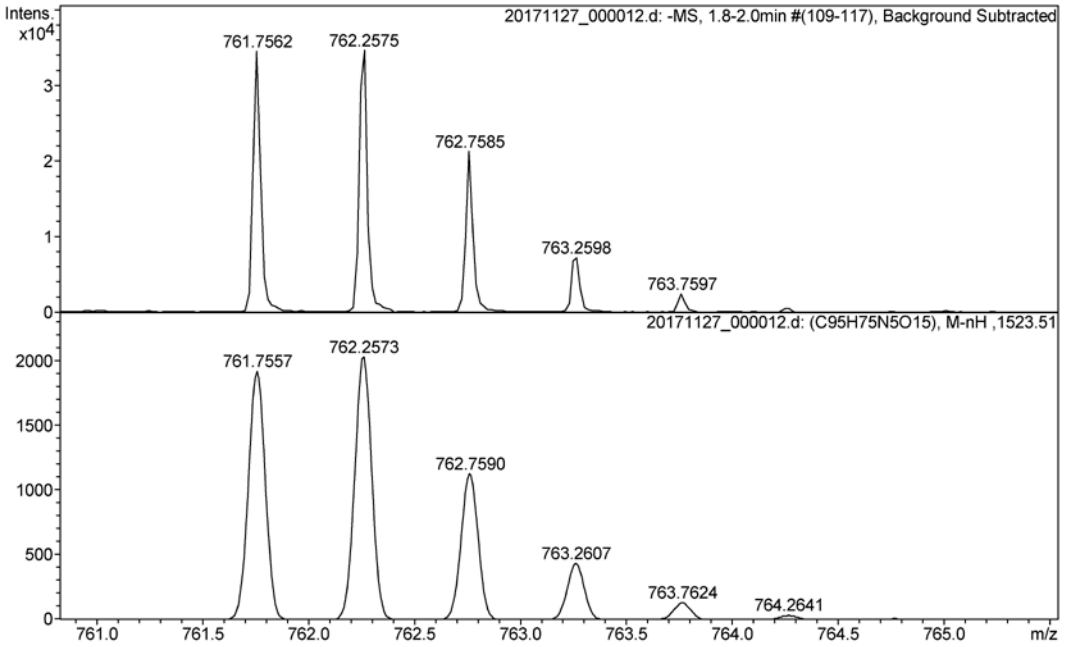

Generic Display Report

Analysis Info

Analysis Name	D:\Data\Agustí Lledó\20171204_000007.d	Acquisition Date	12/4/2017 6:12:48 PM
Method	tune_high.m	Operator	Univ. Girona
Sample Name	DLM013	Instrument	micrOTOF-Q II
Comment			

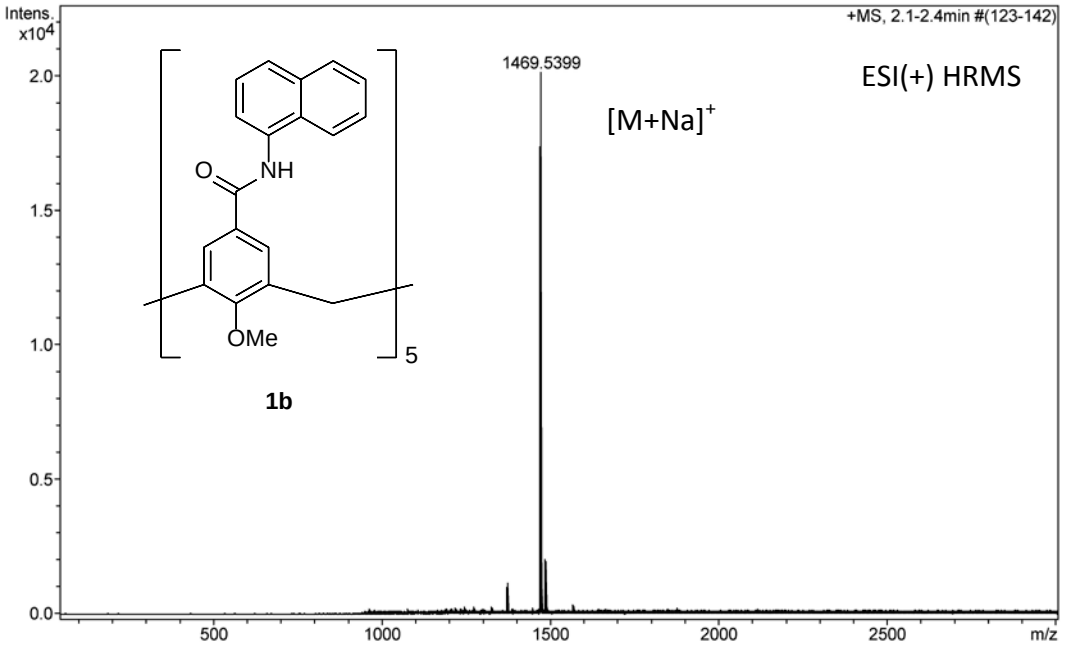

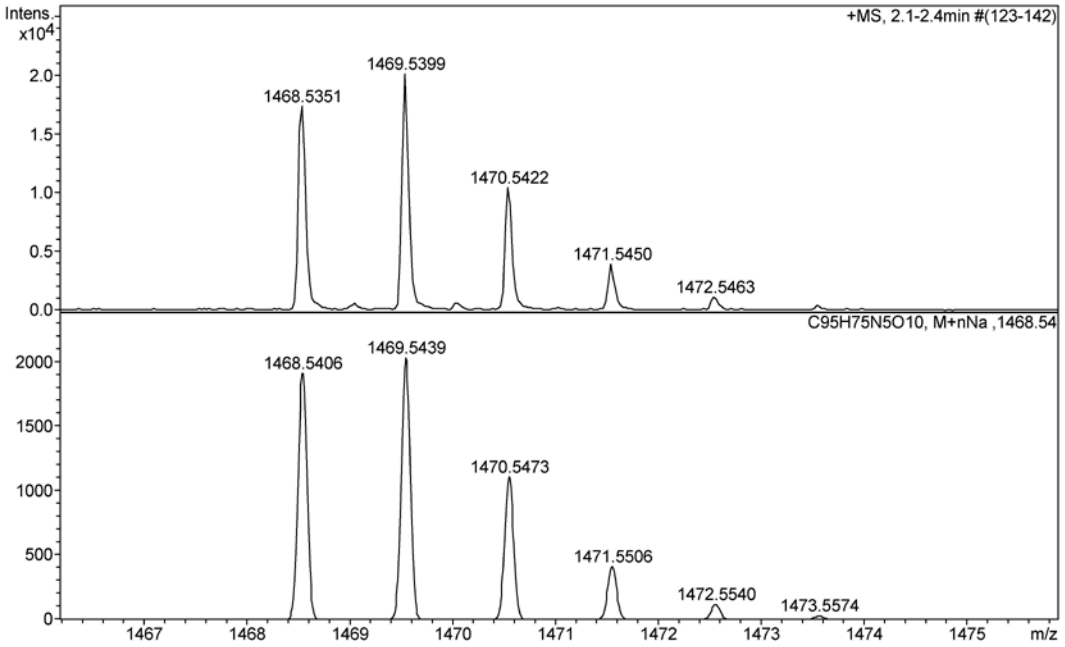

Bruker Compass DataAnalysis 4.0 printed: 12/5/2017 10:32:35 AM Page 1 of 1

Display Report

Analysis Info

Analysis Name	D:\Data\Agustí Lledó\20181023_000004.d	Acquisition Date	10/23/2018 4:51:38 PM
Method	tune_low_negative.m	Operator	Univ. Girona
Sample Name	ALP1469	Instrument	micrOTOF-Q II 10412
Comment			

Acquisition Parameter

Source Type	ESI	Ion Polarity	Negative	Set Nebulizer	0.4 Bar
Focus	Not active	Set Capillary	3500 V	Set Dry Heater	150 °C
Scan Begin	50 m/z	Set End Plate Offset	-500 V	Set Dry Gas	4.0 l/min
Scan End	3000 m/z	Set Collision Cell RF	150.0 Vpp	Set Divert Valve	Waste